Progress in Oceanography

Local and large-scale controls of the exceptional Venice floods of November 2019

--Manuscript Draft--

Manuscript Number:	PROOCE-D-20-00192R1
Article Type:	Full Length Article
Section/Category:	Physical and Geophysical Oceanography
Keywords:	Coastal flooding; PAW surge; Storm Surge; Meteotsunami; Venice
Corresponding Author:	Christian Ferrarin CNR-ISMAR Venice, ITALY
First Author:	Christian Ferrarin
Order of Authors:	Christian Ferrarin
	Marco Bajo
	Alvise Benetazzo
	Luigi Cavaleri
	Jacopo Chiggiato
	Silvio Davison
	Silvio Davolio
	Piero Lionello
	Mirko Orlić
	Georg Umgiesser
Abstract:	On 12 November 2019, an exceptional flood event took place in Venice, second only to the one that occurred on 4 November 1966. Moreover, with four extremely high tides since 11 November 2019, this was the worst week for flooding in Venice since the beginning of sea level records (1872). The event that struck Venice and the northern Adriatic Sea on 12 November 2019, although having certain conditions seemingly typical of the events causing exceptional high waters, had some peculiar characteristics not observed before, that deserved an in-depth analysis. Several factors made this event exceptional: the in-phase timing between the peak of the storm surge and the astronomical tide; a deep low-pressure cyclone over the central-southern Tyrrhenian Sea that generated strong Sirocco (south-easterly) winds along the main axis of the Adriatic Sea, pushing waters to the north; a fast-moving local depression - and the associated wind perturbation - travelling in the north-westward direction over the Adriatic Sea along the Italian coast, generating a meteotsunami; very strong winds (28 m s−1 on average with 31 m s−1 gusts) over the Lagoon of Venice, which led to a rise in water levels and damages to the historic city; and an anomalously high monthly mean sea level in the Adriatic Sea, induced by a standing low-pressure and wind systems over the Mediterranean Sea, that was associated with large-scale low-frequency atmospheric dynamics. In this study, the large set of available observations and high-resolution numerical simulations have been used to quantify the contribution of the mentioned drivers on the peak of the flood event and to investigate the peculiar weather and sea conditions over the Mediterranean Sea during the Venice floods of November 2019.
Suggested Reviewers:	Michael N. Tsimplis M.N.Tsimplis@soton.ac.uk
	Xavier Bertin xavier.bertin@univ-lr.fr
	Ivan David Haigh i.d.haigh@soton.ac.uk

	Arnoldo Valle-Levinson arnoldo@ufl.edu
	Kevin Horsburgh kevinh@noc.ac.uk
Opposed Reviewers:	
Response to Reviewers:	The response to Reviewer's comments and suggestions are included in the attached file.

Highlights

Local and large-scale controls of the exceptional Venice floods of November 2019

Christian Ferrarin, Marco Bajo, Alvise Benetazzo, Luigi Cavaleri, Jacopo Chiggiato, Silvio Davison, Silvio Davolio, Piero Lionello, Mirko Orlić, Georg Umgiesser

- On the 12 November 2019, an exceptional flood event took place in Venice
- Low-frequency disturbances of air pressure and wind provided the longterm precondition for floods
- The resonant coupling of the mesoscale atmospheric forcing and the sea generated a meteotsunami
- Very strong local winds led to a further rise in sea levels and damages to the historic city

Graphical Abstract

Local and large-scale controls of the exceptional Venice floods of November 2019

Christian Ferrarin, Marco Bajo, Alvise Benetazzo, Luigi Cavaleri, Jacopo Chiggiato, Silvio Davison, Silvio Davolio, Piero Lionello, Mirko Orlić, Georg Umgiesser

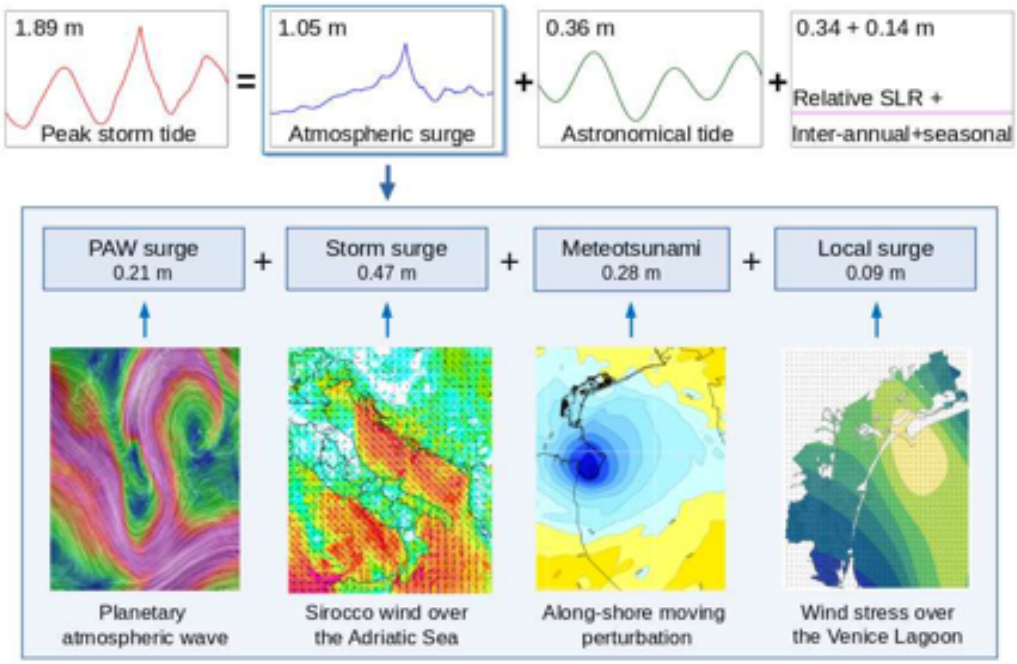

Highlights

Local and large-scale controls of the exceptional Venice floods of November 2019

Christian Ferrarin, Marco Bajo, Alvise Benetazzo, Luigi Cavaleri, Jacopo Chiggiato, Silvio Davison, Silvio Davolio, Piero Lionello, Mirko Orlić, Georg Umgiesser

- On the 12 November 2019, an exceptional flood event took place in Venice
- Low-frequency disturbances of air pressure and wind provided the long-term precondition for floods
- The resonant coupling of the mesoscale atmospheric forcing and the sea generated a meteotsunami
- Very strong local winds led to a further rise in sea levels and damages to the historic city

Local and large-scale controls of the exceptional Venice floods of November 2019

Christian Ferrarin[a,*], Marco Bajo[a], Alvise Benetazzo[a], Luigi Cavaleri[a], Jacopo Chiggiato[a], Silvio Davison[a], Silvio Davolio[b], Piero Lionello[c], Mirko Orlić[d], Georg Umgiesser[a,e]

[a] *CNR - National Research Council of Italy, ISMAR - Marine Sciences Institute, Venice, Italy*
[b] *CNR - National Research Council of Italy, ISAC - Institute of Atmospheric Sciences and Climate, Bologna, Italy*
[c] *Department of Biological and Environmental Sciences and Technologies, University of Salento, Lecce, Italy*
[d] *Department of Geophysics, Faculty of Science, University of Zagreb, Zagreb, Croatia*
[e] *Marine Research Institute, Klaipėda University, H. Manto 84, 92294 Klaipėda, Lithuania*

Abstract

On 12 November 2019, an exceptional flood event took place in Venice, second only to the one that occurred on 4 November 1966. Moreover, with four extremely high tides since 11 November 2019, this was the worst week for flooding in Venice since the beginning of sea level records (1872). The event that struck Venice and the northern Adriatic Sea on 12 November 2019, although having certain conditions seemingly typical of the events causing exceptional high waters, had some peculiar characteristics not observed before, that deserved an in-depth analysis. Several factors made this event exceptional: the in-phase timing between the peak of the storm surge and the astronomical tide; a deep low-pressure cyclone over the central-southern

*Corresponding author. Tel.: +39-041-2407932, Fax: +39-041-2407936
Email addresses: c.ferrarin@ismar.cnr.it (Christian Ferrarin), marco.bajo@ismar.cnr.it (Marco Bajo), alvise.benetazzo@ismar.cnr.it (Alvise Benetazzo), luigi.cavaleri@ismar.cnr.it (Luigi Cavaleri), jacopo.chiggiato@ismar.cnr.it (Jacopo Chiggiato), silvio.davison@ve.ismar.cnr.it (Silvio Davison), s.davolio@isac.cnr.it (Silvio Davolio), piero.lionello@unisalento.it (Piero Lionello), orlic@irb.hr (Mirko Orlić), georg.umgiesser@ismar.cnr.it (Georg Umgiesser)

Tyrrhenian Sea that generated strong Sirocco (south-easterly) winds along the main axis of the Adriatic Sea, pushing waters to the north; a fast-moving local depression - and the associated wind perturbation - travelling in the north-westward direction over the Adriatic Sea along the Italian coast, generating a meteotsunami; very strong winds (28 m s^{-1} on average with 31 m s^{-1} gusts) over the Lagoon of Venice, which led to a rise in water levels and damages to the historic city; and an anomalously high monthly mean sea level in the Adriatic Sea, induced by a standing low-pressure and wind systems over the Mediterranean Sea, that was associated with large-scale low-frequency atmospheric dynamics. In this study, the large set of available observations and high-resolution numerical simulations have been used to quantify the contribution of the mentioned drivers on the peak of the flood event and to investigate the peculiar weather and sea conditions over the Mediterranean Sea during the Venice floods of November 2019.

Keywords: Coastal flooding, PAW surge, Storm surge, Meteotsunami, Venice

1. Introduction

The sea level at a given coastal location is the sum of several contributions, such as mean sea level variability, astronomical tide, changes in sea temperature and the salinity, meteorological surge, seiche, river runoff, and wave setup and run-up, acting on different temporal and spatial scales (Woodworth et al., 2019). Different atmospheric controls on the sea level are characterised by different dynamics, with synoptic and planetary-scale (planetary atmospheric wave, hereinafter PAW) disturbances dominating over periods of a day to a few weeks (storm surge and PAW surge, respectively), while mesoscale forcing are affecting changes occurring at periods lower than a few hours the inertial period (Vilibić et al., 2020). If the response of the sea to air-pressure and wind driven by a mesoscale atmospheric phenomenon surpasses the equilibrium response, a meteotsunami wave is generated. In bays or harbours, such tsunami-like waves can be amplified through the harbour resonance with consequent destructive effects (Vilibić and Šepić, 2009). In semi-enclosed sea, the sea level could also be strongly influenced by sub-daily oscillations (seiche) triggered by storm surges (Cerovečki et al., 1997).

As discussed by Vilibić et al. (2017), all the mentioned components play a role in controlling the sea level variability in the Adriatic Sea, an 800 km long

and 150 km wide elongated semi-closed basin separating the Italian Peninsula from the Balkans and communicating with the Mediterranean Sea only through the Otranto Strait. Storm induced extreme high sea levels occur periodically in the northern Adriatic Sea where they represent the main threat in coastal areas (Lionello et al., 2012). In fact, they can cause a range of potential hazards, such as coastal erosion and inundation, as well as damage to the important cultural heritage exposed to these phenomena. Although several coastal towns can be impacted by sea storms and even flooded, the main concern is for the historical city of Venice in the northern Adriatic Sea, where this phenomenon is known as acqua alta (literally, high water). Severe sea storms in the northern Adriatic Sea are mainly triggered by a strong south-easterly moist and warm wind, called Sirocco, blowing over the whole Adriatic basin (Lionello et al., 2012). Generally, this phenomenology is associated with synoptic situations characterized by an Atlantic trough that, by interacting with the mountain ridges around the Mediterranean Sea while moving eastward, may trigger a secondary cyclogenesis (Buzzi and Tibaldi, 1978; Speranza et al., 1985; Buzzi and Speranza, 1986). Though large storm surges can be produced by cyclones whose main pressure minimum is located above central Europe, the most intense events are caused by well-defined and deep minima above the north-western Mediterranean Sea (Lionello et al., 2005), whose position is particularly effective at causing Sirocco along the Adriatic Sea (Lionello et al., 2012). In fact, the part of the coastline that is most affected by the storm surge depends substantially on the wind structure in the basin (Međugorac et al., 2018). The reader can find in Lionello et al. (2020) a description of the synoptic conditions leading to a high water level in Venice.

The storm we consider in this paper occurred on 12 November 2019, and caused the flooding of about 90% of the city of Venice, thus reaching the second maximum sea level ever recorded in the city (the first maximum was recorded on 4 November 1966). From the first analyses, it appeared clear that the 12 November event was exceptional not only for the flood level reached in Venice but also for the peculiar physical dynamics of the storm (Cavaleri et al., 2020). Although having certain conditions seemingly typical of the events that cause exceptional high waters, the 12 November storm had some peculiar characteristics not observed before that required an in-depth analysis in order to draw conclusions to improve future forecasting and alert systems. In this study, we analyse in situ, remotely sensed and modelled data to perform a detailed investigation of the November 2019 floods and

northern Adriatic Sea dynamics.

The paper is organized as follows. Section 2 presents the large dataset of in situ and remotely sensed data and meteorological and hydrodynamic models used in this study. Section 3 focuses on the dynamics of the 12 November storm in the northern Adriatic Sea. In section 4, we present the results of the analysis of the large-scale and low-frequency dynamics over the Mediterranean Sea, which was responsible for the unusually high mean sea level. Section 5 provides an overview of the sequence of exceptional flooding events that affected the northern Adriatic Sea during the month of November 2019. All this is discussed in section 6 where we also speculate on the statistical significance of the storm as derived from the analysis of long-term sea level records. Conclusions and perspectives are presented in section 7.

2. Methods

2.1. The observational dataset

2.1.1. In situ data

The northern Adriatic Sea and the Lagoon of Venice are well monitored by several meteorological and tide gauge stations (Fig. 1, Ferrarin et al., 2020). Sea level along the western side of the Northern Adriatic Sea is monitored by the Italian tide gauge network (Ancona, Ravenna, Venezia, Caorle, Grado, Trieste) managed by the Institute for Environmental Protection and Research - National Centre for Coastal Zone and Characterization Marine Climatology and for Operational Oceanography (ISPRA), by the Agency for Prevention, Environment and Energy of Emilia-Romagna (Porto Garibaldi), by the Provincia di Ferrara (Goro Faro) and by the National Research Council (the Acqua Alta oceanographic tower - AAOT). The mentioned institutions also manage several coastal meteorological monitoring stations.

The Lagoon of Venice has two tide gauge networks to support the local storm surge prediction and warning system (Fig. 1). They are managed by ISPRA (Unit for Tides and Lagoons, `http://www.venezia.isprambiente.it/` and the Tide Forecast and Early Warning Center of the City of Venice (CPSM, `https://www.comune.venezia.it/it/content/centro-previsioni-e-segnalazioni-maree`).

Water level time series were available for the whole year 2019 at 10 minute intervals; however, multi-year time series have been used when available. Monthly mean and hourly sea level values are available since 1872 and 1940,

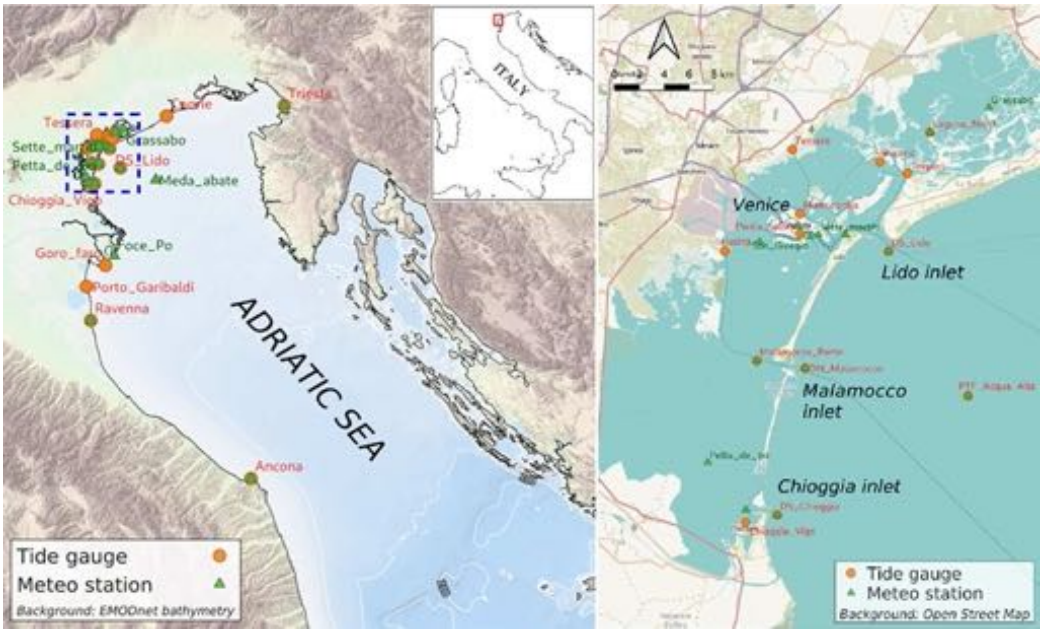

Figure 1: Tide gauges (orange dots) and meteorological monitoring stations (green triangles) in the northern Adriatic Sea (left) and the Lagoon of Venice (right) considered in this study.

respectively, for the tide gauge of Venice Punta della Salute, which is the historical and official reference for the city. Water levels in the Lagoon of Venice are referred to this official datum, corresponding to the mean sea level of the 1885-1909 period. This reference (called ZMPS) is today 0.34 m below the mean sea level (2019 annual mean sea level). All sea level values reported in this manuscript refer to the ZMPS reference (except where explicitly specified).

2.1.2. Remotely sensed data

We used remotely sensed surface wind derived from the Advanced SCATterometer (ASCAT) onboard Metop satellites provided by the Royal Netherlands Meteorological Institute (KNMI), wind speeds from the SSMIS radiometer onboard the F16, F17, F18, and F19 satellites provided by Remote Sensing Systems (RSS), and wind speed and direction from the WindSat radiometer onboard the Coriolis satellite. They have been used as observation inputs for the objective method dealing with the calculation of 6-hourly wind fields over global oceans with 0.25° spatial resolution (`http://marine.`

copernicus.eu/services-portfolio/access-to-products/?option=com_csw&view=details&product_id=WIND_GLO_WIND_L4_NRT_OBSERVATIONS_012_004).

Altimeter gridded (on a 0.125° resolution) sea level anomaly (SLA) is obtained by Optimal Interpolation, by merging the measurement from the different altimeter missions (Pujol et al., 2016) (https://duacs.cls.fr/). Sea level anomaly is computed from the sea surface height measured by altimeters with respect to a twenty-year (1993-2012) mean. In order to account for the wind and pressure contribution to the sea level, the Dynamic Atmospheric correction (DAC), which is routinely applied to remove high-frequency variability induced by the atmospheric forcing from the altimetric measurements, has been added to the SLA products. DAC is computed as the combination of high-frequency elevations from the Mog2D/T-UGOm barotropic model simulation forced by atmospheric pressure and winds (Carrère and Lyar, 2006), plus low-frequency elevations from inverted barometer effect (using ECMWF atmospheric pressure products).

2.2. Data analysis

2.2.1. Sea level decomposition

Tide gauge time series were processed with a tidal harmonic analysis tool based on the least squares fitting (Codiga, 2011) to separate the tidal and the non-tidal contributions to the total sea level. Even if seven tidal constituents provide the most significant contribution to the tidal level elevation in the Adriatic Sea (Polli, 1960), the method determines the components that are computable according to the record length (thus considering also long-term tides in the multi-year records), considers the nodal correction and can deal with an incomplete series of data.

Once this decomposition of the total sea level has been carried out, we aim at identifying the different atmospheric processes responsible for what we call meteorological and mean contribution, based on their time-frequency range. The transition between different processes is smooth, i.e. the spectrum of atmospheric variability is mostly continuous. However, it is still possible to distinguish between various processes contributing to the continuum due to their relationship with the mid-latitude atmospheric phenomena. Most often, the distinction is made on the basis of different space scales of the phenomena. Among a number of classifications developed for the purpose, one of the simplest appears to be that proposed by Holton (2004): he makes distinction between the planetary-scale motions, of O(10^7 m), the synoptic-scale

motions, of O(10^6 m), and the mesoscale motions, of O(10^4 m) - O(10^5 m). Moreover, he points out that the planetary atmospheric waves tend to move westward against the eastward zonal flow and are therefore characterized by relatively small speeds (1-10 m s^{-1}) whereas the synoptic-scale systems tend to move eastward in the mean flow and are consequently marked by relatively large speeds (typically 10 m s^{-1}). As for the mesoscale systems, their speeds are also relatively large, i.e. of the order of 10 m s^{-1} (Markowsky and Richardson, 2010). By allowing for these space scales and speeds, it is easy to show that the time scales of various processes also differ, being for the planetary-scale motions of O(10 days) - O(100 days), for the synoptic scale motions of O(1 day), and for the mesoscale motions of O(10 minutes) - O(1 hour). The differences between the space and time scales and the related speeds reflect the different dynamics controlling the atmospheric phenomena. At the planetary scale, the Rossby wave dynamics prevails. At the synoptic scale, motions are mostly driven by baroclinic instability. Mesoscale processes are either topographically forced or are driven by one of a number of instabilities operating at that scale.

Having in mind the stated time scales, in order to estimate the different meteorological contributions to the sea level (inter-annual and seasonal variability, PAW surge, storm surge, high-frequency oscillations), we then have applied digital filters (low-pass, band-pass and high-pass, as listed in Table 1) in the spectral domain assuming Fourier decomposition. The approach is similar to the one previously followed by Orlić (2001).

Table 1: Cut-off periods used in the data analysis to separate the different atmospheric contributions to the total sea level.

Atmospheric contribution	*Type of filter*	*Cut-off periods*
Inter-annual and seasonal variability	Low-pass	$>$ 120 days
PAW surge	Band-pass	10 - 120 days
Storm surge	Band-pass	10 hours - 10 days
High-frequency oscillations	High-pass	$<$ 10 hours

The selection of filters is further supported by previous findings. The value separating synoptic scale and planetary scale is close to 10 days (Pasarić et al., 2000); the corresponding one for meso-scale and synoptic scale is ca. 10

hours (Šepić et al., 2012). Orlić (1983) has performed cross-spectral analysis of the geopotential height of 500 hPa surface above the Adriatic and the sea level. The results showed that the coherence is high at periods surpassing 10 days (at which planetary-wave dynamics dominates) and is much weaker at periods smaller than 10 days (at which baroclinic instability operates). On the other hand, Markowsky and Richardson (2010) have stated that the time scales of mesoscale atmospheric phenomena range from the period of a pure buoyancy oscillation (roughly 10 minutes) to the inertia period (roughly 17 hours in midlatitudes). Moreover, the seasonal signal differs from the planetary wave signal, the former being related to a line in the spectrum of atmospheric variability, the latter belonging to a continuous part of the spectrum. The separation between the PAW signal and the seasonal (and inter-annual) cycle was achieved by applying a low-pass filter with the cut-off period placed at 120 days. The filters were applied to the sea level time series as well as to the meteorological model fields (for each point of the model domain) to synthesise the different meteorological contributions to sea level through numerical experiments.

2.2.2. Extreme sea level analysis

Extreme value analysis was performed on the hourly 1940-2019 sea level timeseries of Punta della Salute. In general, there are two main families of methods for extreme sea level analysis. Classical direct methods, such as the annual maxima, the peak-over-threshold and the r-largest approaches, deal with the total sea level variable by directly analyzing the set of observed stochastic variables. Indirect methods, on the other hand, model the tidal and non-tidal residual components separately, considering the astronomical tide as a fully deterministic variable and the surge as a stochastic one. In this case. the total sea level extremes are then inferred by recombining the two components by means of convolution of the empirical distributions. The two most widely used indirect methods are the joint probability method (JPM, Pugh and Vassie, 1980) and the revised joint probability method (RJPM, Tawn and Vassie, 1989). The reader is referred to Haigh et al. (2010) for an overview and comparison of the aforementioned statistical methods.

In the context of our work, we have decided to use both methods, as the indirect one allows us to effectively separate the two main contributions of tide and non-tidal atmospheric residual. Of the two cited indirect methods, we have regarded the JPM as the simplest yet effective tool for our area of interest, as explained in the following. For the computation of the tidal level

distribution, we define a support of its distribution covering the entire range of tidal level values at discrete intervals (taken to be equal to the measurement accuracy, i.e. 0.01 m), with the smallest value lower than the Lowest Astronomical Tide and highest value higher than the Highest Astronomical Tide. The empirical density function of the tidal level is then defined over said support using a kernel density estimator, setting the probability to zero for values outside the bounded support. The same procedure is also applied to the non-tidal residual observations. Once again, a null probability is assumed for surges larger than the highest observation, thus assuming that the available record is a representative sample of the population of all possible residual values.

While this procedure may be appropriate for the deterministic component (i.e. tide), it may, on the other hand, lead to underestimations for the stochastic part, particularly for the extreme values, which are few and subject to large variability (Tawn and Vassie, 1989; Mazas et al., 2014). In this sense, the RJPM method would enable probabilities beyond the existing value range of the data as well as a smoother tail of the empirical distribution to be obtained. While being fully aware of the improvements of such method, also shown in Mazas et al. (2014), for the present study it was assumed that the empirical distribution is a good approximation of the true distribution, given the 80-year extent of the used dataset.

Once the probability density function of the total sea level is estimated, the cumulative distribution function can easily be derived, which, although more appropriate, may not be as easy to understand as the return period. However, the definition of the return period for hourly sea levels is not straightforward because of the autocorrelation present in the hourly sea level sequence, due to the temporal dependence that both tide and surge exhibit (e.g. clustering of surge events, each often persisting for several hours). Classical definitions of return periods that treat each value as independent can thus be critical in the case of surge-dominant sites such as the area of interest and will tend to produce overestimates (Tawn and Vassie, 1989). In this respect, the application of the RJPM method would fully account for the dependence in the hourly data, as it uses an extremal index derived from the mean overtopping time of a level for each independent storm that exceeds that level. However, our interest in this work is not the quantification of the return periods, rather the frequency with which the convoluted sequence might exceed (or not exceed) a given extreme level relative to other measured levels. For this reason, we have decided to use the concept of "ex-

ceedance interval", which retains the simplicity of the return period concept and preserves its strength in indicating the probability of a certain event. The expression of the exceedance interval coincides with the return period for the case of independence in time, as in Pugh and Vassie (1980).

2.3. Modelling approach

In this section, we describe the meteorological and oceanographic models used to simulate the storm dynamics. For a clear understanding of the modelling approach, we provide a detailed description of the model applications and set-up for the Mediterranean Sea and the Lagoon of Venice.

2.3.1. Meteorological modelling

In order to reproduce the meteorological situation of 12 November, we performed a dynamic downscaling of global ECMWF reanalysis ERA5 fields to an adequate space-time resolution for the local simulations. ERA5 is the latest climate global reanalysis produced by ECMWF, providing hourly data on regular latitude-longitude grids at 31 km (0.28125 degrees) resolution (Hersbach et al., 2020). Reanalysis combines model data with worldwide observations into a globally complete and consistent dataset using an advanced data assimilation method, based on 4D-Var. ERA5 reanalysis data are available from the Copernicus Climate Data Store (`https://climate.copernicus.eu/`).

In this study, the meteorological downscaling is supplied by the MOLOCH non-hydrostatic, fully compressible, convection-permitting model (Malguzzi et al., 2006). The prognostic variables, namely pressure, air temperature, specific humidity, horizontal and vertical wind velocity components, turbulent kinetic energy and five water species, are represented on a latitude-longitude rotated Arakawa C-grid. It employs a height-based hybrid coordinate, relaxing smoothly to horizontal surfaces away from Earth's surface. Time integration is based on a time-split scheme with an implicit treatment of the vertical propagation of sound waves and a forward-backward scheme for the horizontal propagation of gravity and sound waves. The three-dimensional advection scheme is based on a second-order, weighted-average flux implementation with superbee limiter (Hubbard and Nikiforakis, 2003). See Buzzi et al. (2014) and Davolio et al. (2017) for further details about the MOLOCH model physics and numerics.

In the operational practice, as well as for this study, the MOLOCH model is implemented with a horizontal grid spacing of 0.0113 degrees, equivalent

to 1.25 km, and with 60 atmospheric levels and 7 soil levels over a numerical domain comprising the Italian peninsula and the adjacent seas (including the whole Adriatic Sea). To minimise the error of the modelling system (due to spin-up or long forecast lead time), but at the same time to enable a dynamic downscaling, we concatenated a series of short-range simulations of MOLOCH, in the range between +6h and +12h obtained by nesting MOLOCH into ERA5 hourly analysis. Subsequently, the MOLOCH outputs were merged with the ERA5 fields over the rest of the Mediterranean Sea in order to cover the whole domain of the hydrodynamic modelling system (see section 2.3.2), similarly to the procedure applied in Ferrarin et al. (2013). Several tests were initially performed to ensure the absence of significant discontinuities between subsequent time steps and at the boundaries between MOLOCH and ERA5.

The MOLOCH simulations covered the whole period between 10 and 13 November 2019. The MOLOCH-ERA5 meteorological fields were elaborated to separate the different atmospheric contributions considering the cut-off periods reported in Table 1. Moreover, to obtain consistent wind and air pressure fields for the hydrodynamic simulations, low-pass filters with the cut-off period of 10 days (aimed at removing storm surge and meteotsunami signals) and 10 hours (aimed at removing only the meteotsunami signal) were also produced.

2.3.2. Hydrodynamic simulation experiments

The numerical experiments consisted of simulating the circulation in the Mediterranean Sea and the Lagoon of Venice using the open-source 3D finite element SHYFEM hydrodynamic model (`https://github.com/SHYFEM-model/shyfem`). The model has been already applied to simulate hydrodynamics in the Mediterranean Sea (Ferrarin et al., 2013), in the Adriatic Sea (Bajo et al., 2019) and in several coastal systems (see Umgiesser et al., 2014, and reference therein). The model solves the shallow-water equations in their formulations with levels and transports using a finite-element numerical method and semi-implicit time stepping. The Coriolis term and pressure gradient in the momentum equation and the divergence terms in the continuity equation are treated semi-implicitly. Bottom friction and vertical eddy viscosity are treated fully implicitly for stability reasons due to the shallow nature of the lagoon, while the remaining terms (advective and horizontal diffusion terms in the momentum equation) are treated explicitly. A detailed description of the 3D model equations is given in Umgiesser et al.

(2014) and Bellafiore et al. (2018).

The storm surge contribution in the Adriatic Sea is evaluated with the SHYFEM model over a spatial domain covering the Mediterranean Sea, the Adriatic Sea, the Po Delta and the northern Adriatic lagoons by means of an unstructured grid consisting of approximately 267,000 triangular elements. Mesh resolution varies from 12 km in the open sea to a couple of km in coastal waters and up to few meters in the narrow channels inside the lagoons (Fig. 2). Model bathymetry over the Mediterranean Sea is obtained by a bilinear interpolation on the model grid of the European Marine Observation and Data Network (EMODnet) 2016 dataset (`http://www.emodnet-bathymetry.eu`). The Adriatic Sea could be formally subdivided based on its bathymetry in a relatively shallow northern Adriatic (depths are in the order of few tens of meters), the mid-Adriatic Pit (depths up to about 200 m) and the deep southern Adriatic Pit (with depths exceeding 1,000 m).

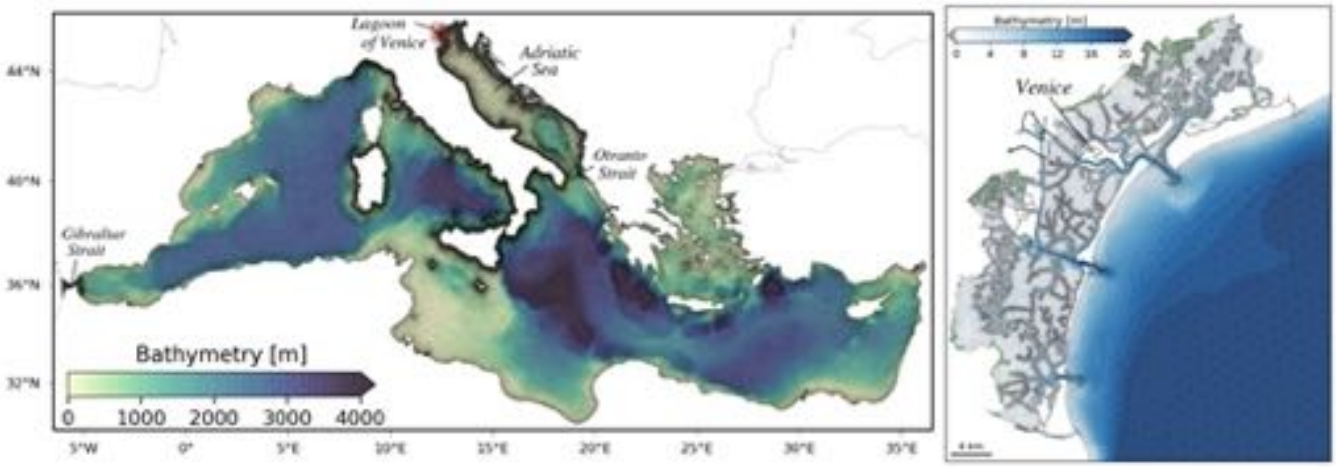

Figure 2: Unstructured model grid and bathymetry of the Mediterranean Sea and a zoom (right panel) over the Lagoon of Venice.

The model adequately reproduces the complex geometry and bathymetry of the Lagoon of Venice using unstructured numerical meshes composed of triangular elements of variable form and size (right panel in Fig. 2). The model bathymetry for the Lagoon of Venice was obtained from the data collected in 2002 by Magistrato alle Acque di Venezia - merged with later surveys - and the 2014 MBES bathymetry acquired by CNR-ISMAR in the

main channels of the lagoon (Madricardo et al., 2017). The application of the SHYFEM model to the Lagoon of Venice has been validated in previous works reproducing correctly tidal propagation, storm surge, water flows at the lagoons' inlets and water temperature and salinity variability (Ferrarin et al., 2010).

Sea level boundary conditions at the Gibraltar Strait are provided by the IBI forecasting system (Sotillo et al., 2015). At the sea surface, SHYFEM was forced with wind and atmospheric pressure fields produced by ERA5 reanalysis and MOLOCH. A spin-up period of one month from 10 October to 10 November 2019 was considered with the SHYFEM model forced by ERA5 fields. Sea level and currents fields on 10 November at 00:00 UTC were used as initial conditions for the hydrodynamic simulations throughout the peak of the storm. These numerical experiments were forced by the composite MOLOCH-ERA5 fields for the period from 10 to 12 November. In order to analyse different meteorological contributions to sea level, we performed several numerical experiments with SHYFEM applied over the Mediterranean Sea domain and forced by filtered meteorological fields using different frequency ranges. An additional simulation of the storm peak was performed considering the ERA5 forcing over the whole Mediterranean Sea in order to investigate the effect of the meteorological dynamical downscaling on the sea level.

The water circulation in the Lagoon of Venice, induced by the storm tide and the wind, was simulated also separately by applying SHYFEM over a spatial domain that represents the entire lagoon up to the inlets. In this last simulation, SHYFEM ran coupled with the WWMIII spectral wave model (Roland et al., 2009) and was forced by wind fields obtained from observations at different stations (Fig. 1), which were interpolated with Gaussian weights over a regular grid covering the lagoon. The sea level imposed at the three lagoon's inlets was also obtained directly from observations, in order to obtain the most accurate simulation possible. This model configuration was run for the period from 8 to 15 November 2019, considering the first 4 days as a spin-up period. For analysing the effect of the local wind on the sea level inside the lagoon, the results of this simulation were compared to those of a simulation without wind forcing.

3. The 12 November storm

3.1. General meteorological framework

Due to the particular shape and orography - with the Alps to the north, the Dinaric Alps to the east and the Apennines to the west - winds in the Adriatic Sea are strongly influenced by local, orographic features (Pasarić et al., 2009). This condition was plain on 12 November, when a deep low-pressure cyclone over the central-southern Tyrrhenian Sea (L1 in Fig. 3) generated strong Scirocco (south-easterly) winds along the main axis of the Adriatic Sea, while, at the same time, Bora (north-easterly) winds blew over the northern Adriatic. This synoptic configuration is normally the cause of high sea level events in the Lagoon of Venice, with the Scirocco wind pushing the Adriatic waters to the north and the Bora wind that locally deflects the accumulation towards the western coasts. In addition to this large-scale configuration, the northern Adriatic was affected by the passage of a small-scale cyclonic vortex (L2 in Fig. 3), which travelled over the sea almost parallel to the Italian coast, from central Italy to the northern Adriatic basin, in the afternoon of 12 November.

The passage of the cyclonic vortex L2 is clearly evident from the data measured at AAOT, located in the Gulf of Venice, 15 km offshore the Venetian littoral (Cavaleri, 2000). As can be seen in Fig. 4, the arrival of the warm front, accompanied with the increase in the air temperature of 5-6 °C, and the rapid descent of the air pressure (about 3 hPa in half an hour), are clearly displayed in the data until the minimum pressure value (986.6 hPa) transited at 20:30 UTC. Subsequently, a cold front impressed a rotation of the winds to south-westerlies, with a severe intensification of wind speed (up to 26 m s^{-1} on average and 33 m s^{-1} gusts) and a drop of 5-6 °C in the air temperature.

The high-resolution MOLOCH model results displayed in Fig. 5 clearly show that the rapid deepening of this small-scale low-pressure system (L2) while moving northward. The L2 depression was located north of Ancona on 12 November at 15 UTC and it propagated northward towards Venice where it arrived at 21:30 UTC. The speed of L2 moving northward was estimated to be about 12.5 m s^{-1}. The model results indicate the presence of the warm front, with south-easterly wind, on one side and cold north-easterly winds over the northern Adriatic Sea (Fig. 5 at 17 UTC).

The satellite data retrieved by the ASCAT scatterometers in the northern Adriatic Sea on 12 November at 19:00 (Metop-A) and 19:40 UTC (Metop-C)

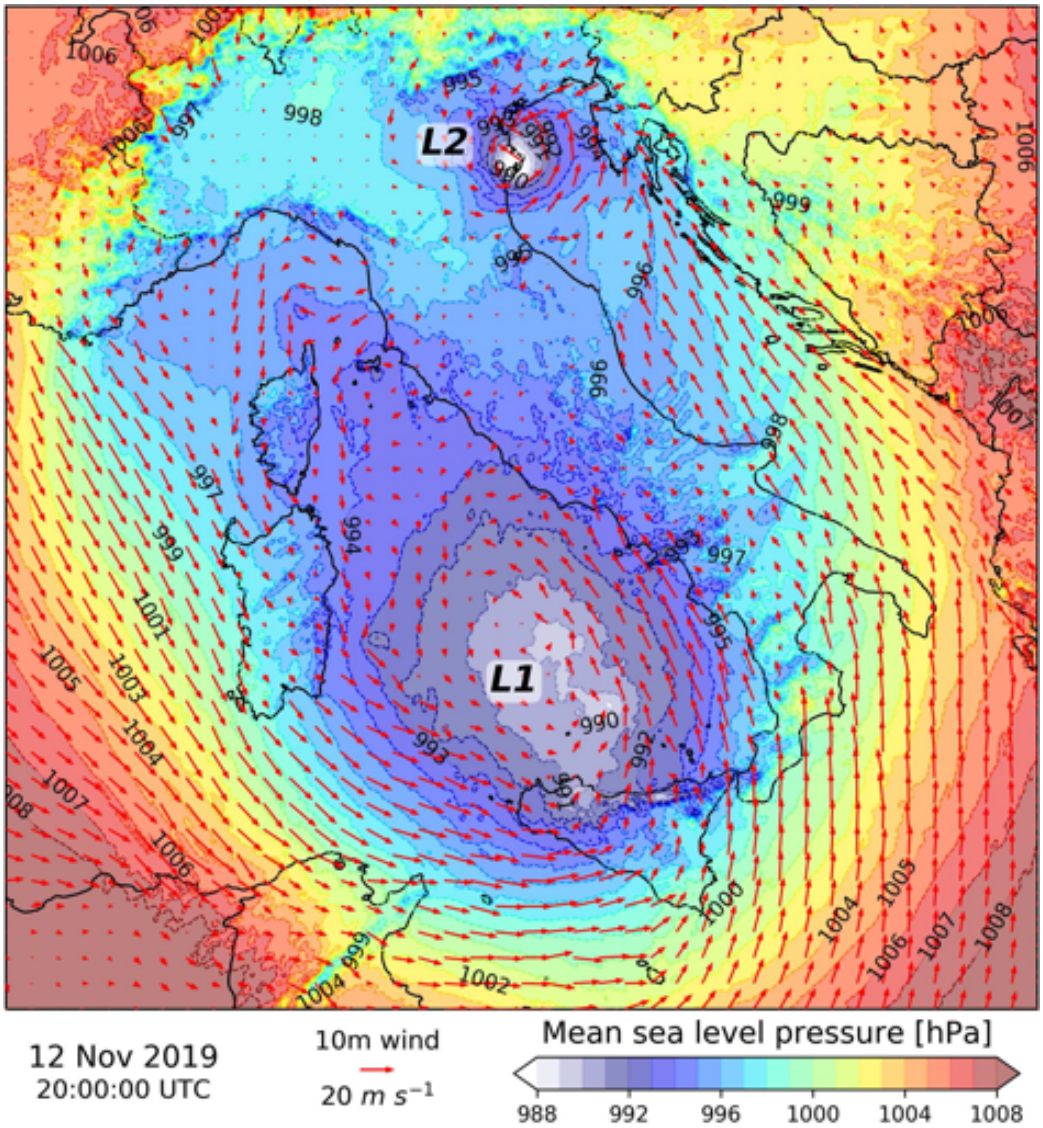

Figure 3: Mean sea level pressure (colour shade and isolines) and 10m wind (arrows) simulated by the MOLOCH model on 12 November at 20:00 UTC. Labels L1 and L2 indicate the two low-pressure systems.

indicate the presence of a perturbation moving northward with wind speed exceeding 20 m s^{-1} (Fig. 6). The MOLOCH model reproduced reasonably well the dynamics and strength of the cyclonic circulation vortex detected by the scatterometers in the northern Adriatic Sea. With respect to the

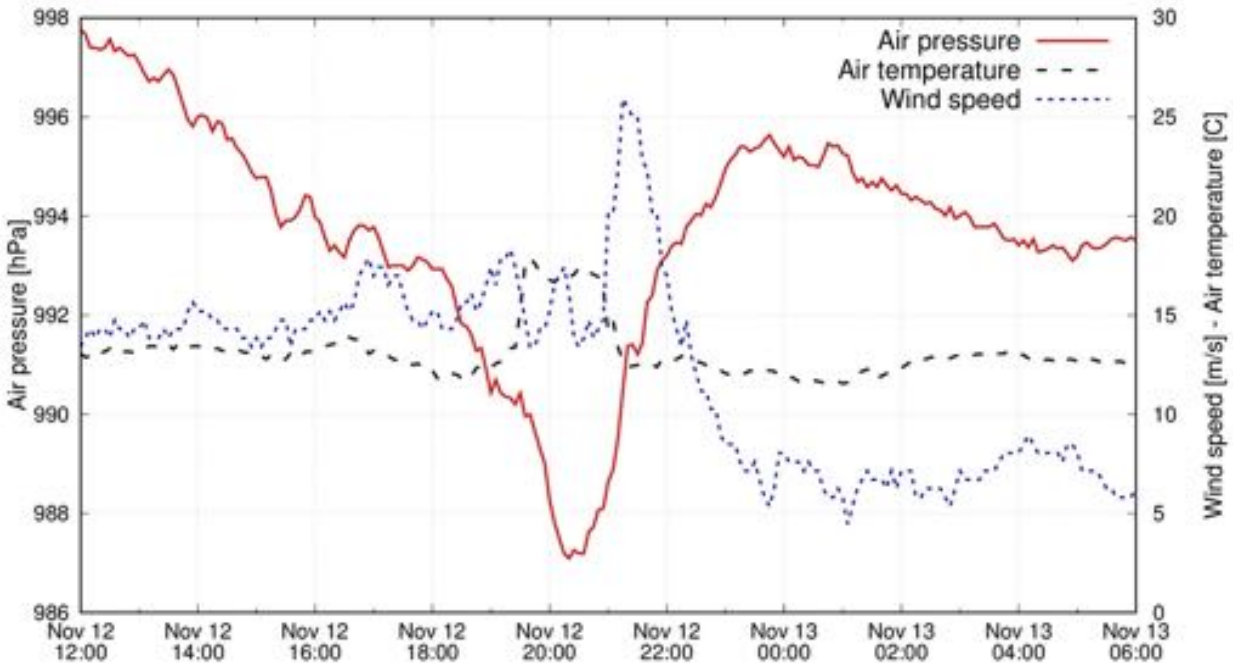

Figure 4: Mean sea level pressure, air temperature and mean wind speed recorded at the Acqua Alta tower.

observations, the MOLOCH model places the vortex slightly closer to the Italian coast.

The improvements of the reanalysis fields obtained by means of the dynamic downscaling with the MOLOCH model emerged through the comparison with the in situ observations. Figure 7 shows that ERA5 strongly underestimates the pressure minimum, while the MOLOCH model reproduces well the passage of the deep perturbation moving along the Italian coast. The improvements were mainly due to the high-resolution of the limited area model, which allows to reproduce the small-scale processes, including convection and interaction with the complex orography, possibly responsible for the development of the mesoscale vortex. The lack of observations over the sea and the relatively coarse resolution of ERA5 prevented a correct description of the small-scale cyclonic vortex in the reanalysis fields. Similarly, the air pressure and associated wind fields produced by the ECMWF Tco1279 operational model forecast were substantially underestimated (Cavaleri et al., 2020).

The mismatch in the track of the perturbation simulated by ERA5-

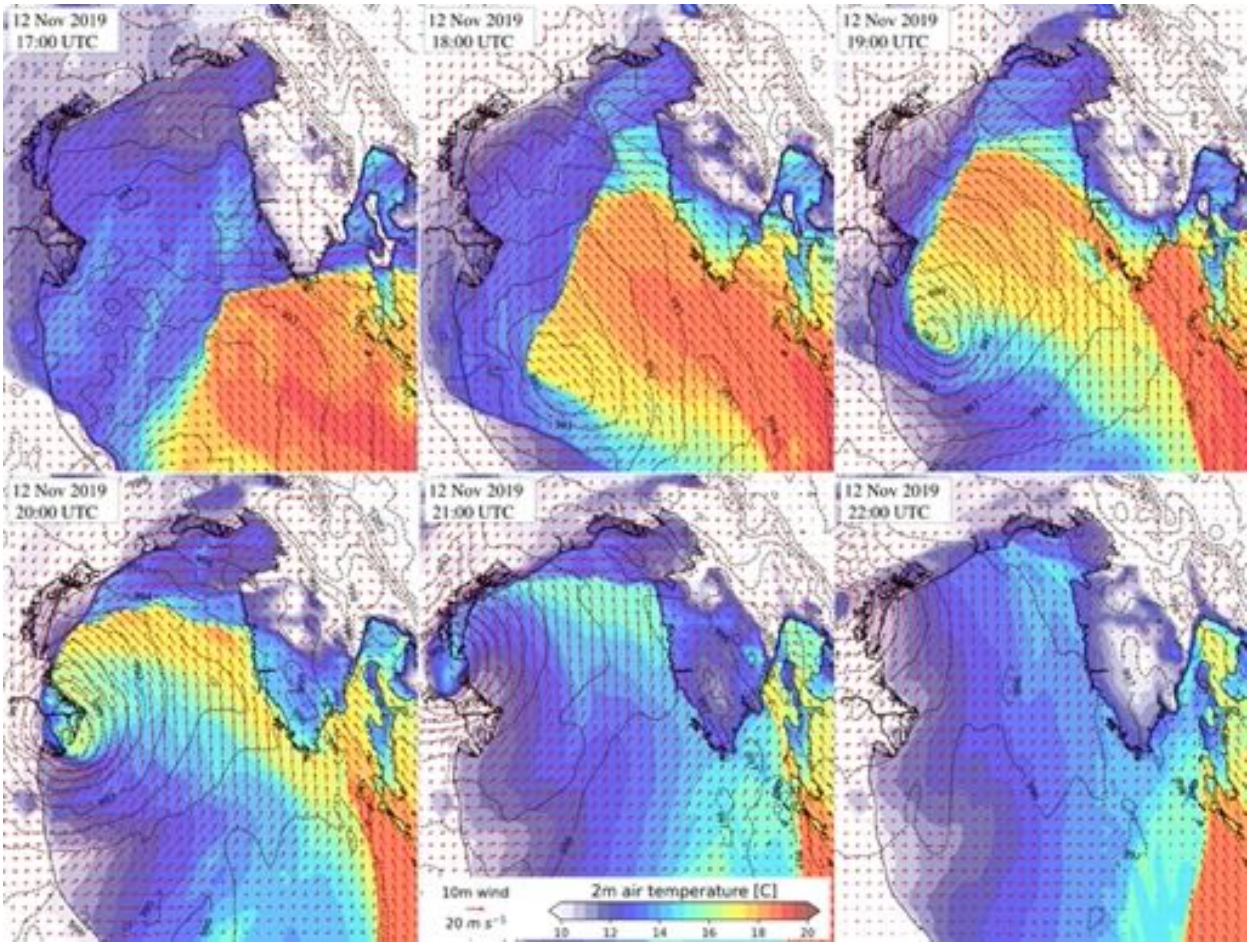

Figure 5: Mean sea level pressure (isolines), 2 m air temperature (colours) and 10 m wind (arrows) simulated by the MOLOCH model over the northern Adriatic Sea during the evening of 12 November 2019.

MOLOCH is confirmed by the comparison of the model results with a series of coastal meteorological stations, including those at AAOT. The spatial interpolation of the recorded wind data (Fig. 8) suggests that the minimum remained near to the coast and crossed one of the lagoon's barrier islands, about 10 km west of Venice, while the model shows that the perturbation passed over the Po Delta and then moved inland keeping the lagoon on its right. Similarly, the predicted path of the depression was shifted also in the ECMWF forecasts (Cavaleri et al., 2020). Over the lagoon, the wind obser-

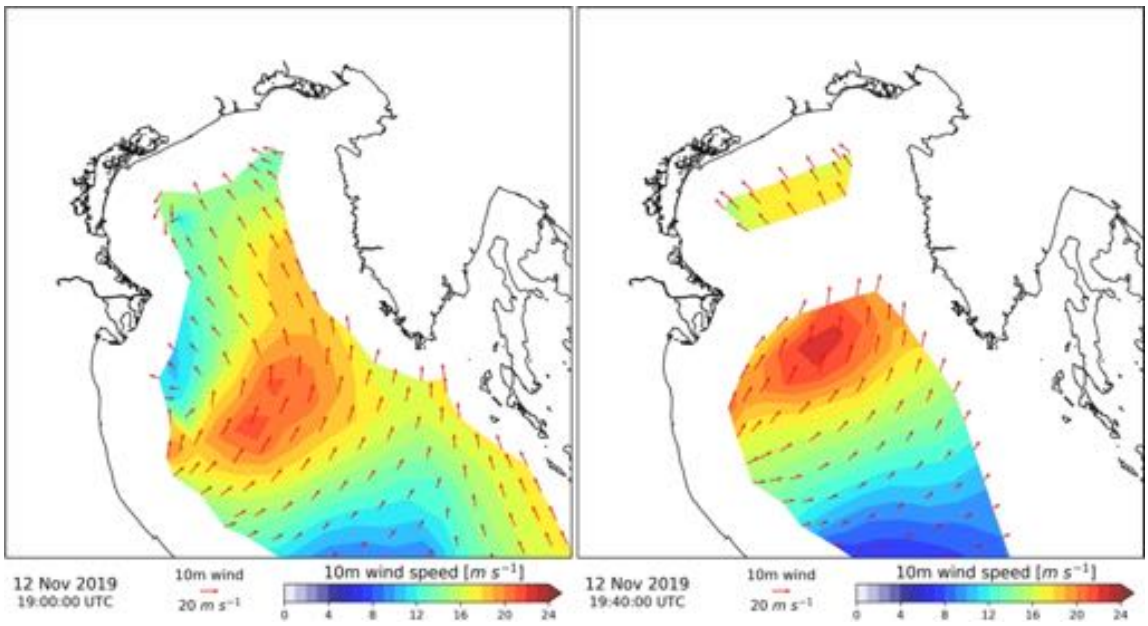

Figure 6: Scatterometer wind fields at 19:00 (Metop-A) and 19:40 (Metop-C) UTC on 12 November 2019.

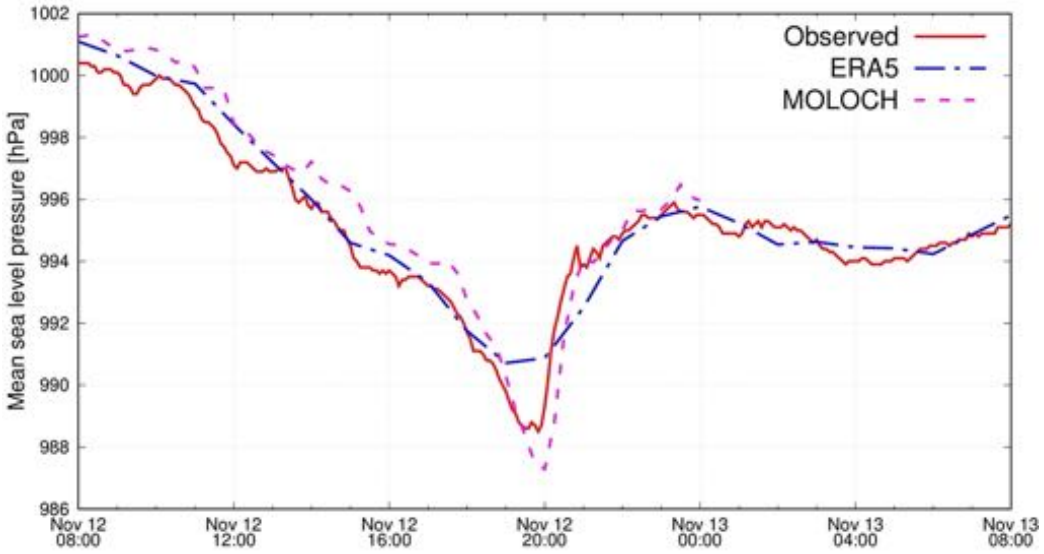

Figure 7: Observed and modelled (ERA5 and MOLOCH) mean sea level pressure at Foce Po.

vations reached maximum values of 28 m s^{-1} on average and 31 m s^{-1} gusts at 21:30 UTC.

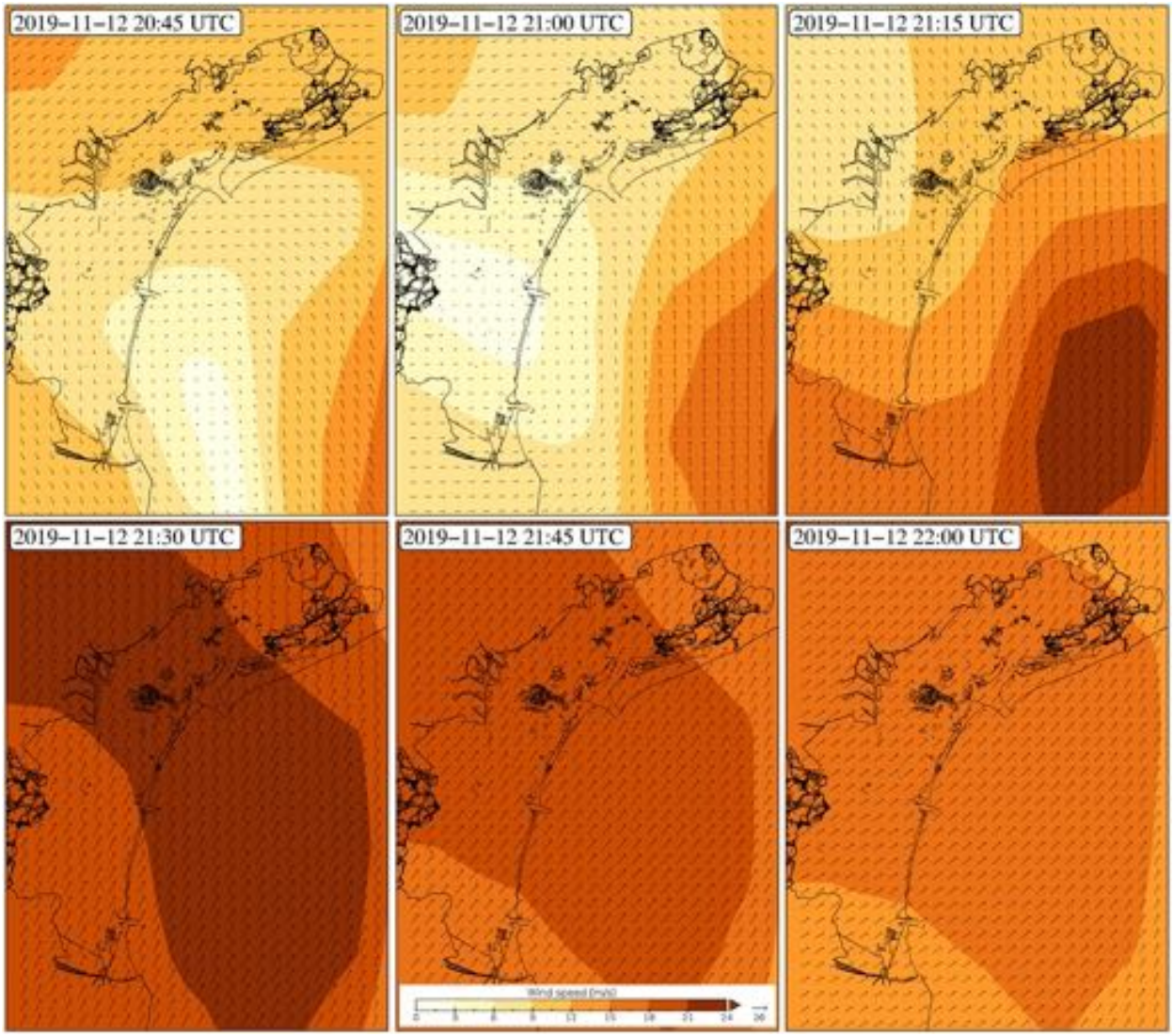

Figure 8: Wind fields over the Venice Lagoon obtained by the optimal interpolation of the observations.

The spectral analysis of the simulated meteorological fields allowed to separate the different meteorological contributions (Fig. 9). The long-term signal (Fig. 9a, obtained by a low-pass filter with the cut-off period of 10 days)

revealed a large-scale dynamics with south-easterly winds over the southern and central Adriatic with speed in the order of 8 m s^{-1}. The band-pass filter selecting the signal with a period ranging between 10 days and 10 hours extracted the main L1 perturbation which generated strong winds over the central Mediterranean Sea (up to 15 m s^{-1}) and south-easterly and easterly winds in the Adriatic Sea (Fig. 9b). The remaining simulated high-frequency contribution (Fig. 9c), which considers the signal with periods lower than 10 hours, represents the local small-scale perturbation characterized by a 3-4 hPa depression and strong winds (above 18 m s^{-1}) in the northern Adriatic Sea and over the Lagoon of Venice.

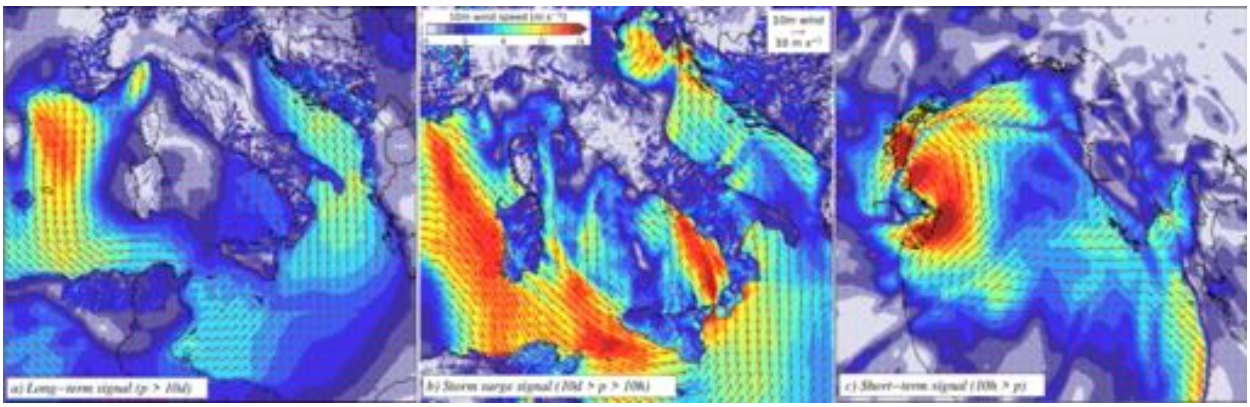

Figure 9: a) Long-term (over the central Mediterranean Sea), b) storms surge (over Italy) and c) High-frequency (over the northern Adriatic Sea) wind fields obtained by the spectral analysis of the MOLOCH-ERA5 meteorological model results (12 November at 20:30 UTC).

3.2. Sea level evolution in the Adriatic Sea

Observations acquired at AAOT provided a clear overview of the sea conditions in the northern Adriatic Sea (offshore the lagoon of Venice) during the 12 November storm. As shown in Fig. 10, the maximum sea level value of 1.82 m was recorded at 20:40 UTC. The exceptionally high water was determined by sheer coincidence of the maximum residual contribution (1.45 m) with the lower high tide (0.37 m). It has to be noted that fluctuations of the northern Adriatic Sea level at tidal frequencies are among the most important of the entire Mediterranean Sea (Tsimplis et al., 1995). A few important remarks must be acknowledged. The annual mean sea level in

2019 in the northern Adriatic was 0.34 m, while the mean in November was anomalously high (0.67 m). It is also important to specify that, although the sea level in Venice was the 2^{nd} highest ever recorded, the residual contribution on 12 November was lower than the maximum residual contributions recorded during the remarkable events of 1966 and 2018 (De Zolt et al., 2006; Cavaleri et al., 2019).

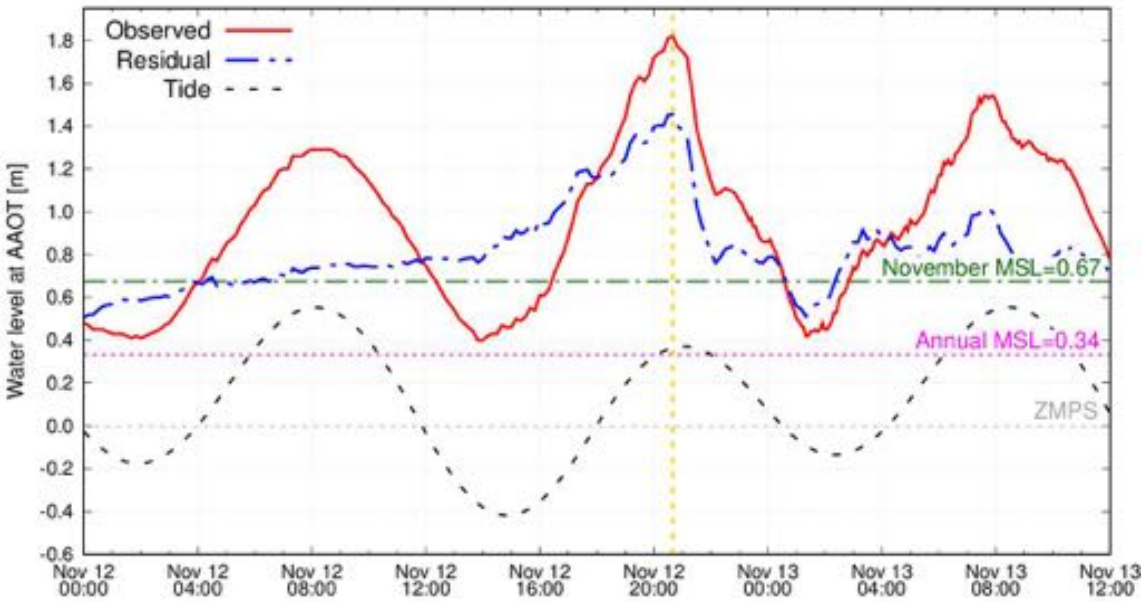

Figure 10: Observed, residual and tidal levels at the AAOT. 2019 annual and November mean sea levels are reported with dotted magenta and dash-dotted green horizontal lines, respectively. The vertical yellow dashed line highlights the time of the peak of the total and residual water level.

The residual sea level (obtained by subtracting the tide from the total water level) was further analysed to investigate the role of the different processes determining the peak flood level. The spectral analysis performed according to the cut-off period listed in Table 1 and presented in Fig. 11 allows us to separate the sea level signal into the following components:

- long-term signal accounting for the relative sea level change, seasonal oscillation and inter-annual variability with a value of 0.48 m (referred to the ZMPS reference datum);
- PAW surge mainly triggered by meteorological perturbation in the

range of planetary atmospheric waves, with an almost constant value of 0.21 m;

- storm surge, induced by air pressure gradients and south-easterly winds associated with the L1 perturbation over the Tyrrhenian Sea, with a maximum of 0.57 m at AAOT. It is important to note that the peak of the L1 storm surge level occurred around 19:00 UTC, about one and a half hours before the peak of the total sea level (when the storm surge equalled 0.47 m; such value includes a small seiche oscillation of about 0.05 m);

- high-frequency oscillation (in the meteotsunami-like frequency band) which could be associated with the air pressure minimum and strong wind generated by the fast moving perturbation L2, with a maximum of 0.28 m at the moment of the peak sea level. Afterwards, the high-frequency signal displays a series of oscillations having a periodicity of about 4 hours, probably related to cross-basin seiches of the North Adriatic Sea (Stravisi, 1977) triggered by the L2 perturbation.

The analysis of the sea level records acquired along the Italian coast allowed us to draw a picture of the effect of the meteorological contributions to the 12 November storm. Following the L2 perturbation from south to north, we present in Fig. 12 the residual sea levels registered at different stations. Under the effect of the Sirocco wind, the sea level north of Ancona rose till the evening of the 12 November. An anomalously fast drop of the sea level occurred around 20:00 UTC, reaching about 0.80 m at the monitoring stations located south of the Po Delta (Porto Garibaldi and Goro Faro). After reaching the minimum at around 21:00 UTC, the sea level rose again to a value similar to the one before the anomaly. Such a fast "V shape" oscillation, which lasted only two hours, occurred following the passage of the small-scale perturbation L2. An analysis of meteorological observations along the coast suggests that a sudden drop of the Adriatic Sea level south of the Po Delta could have been the consequence of strong westerly winds blowing (for almost a couple of hours) from the coast offshore. Besides the effect of the wind stress, the transport of cold air generated by evaporative cooling over the Po valley and at the foot of the Apennines where convective activity persisted in the afternoon, produced a rapid increase in surface pressure.

Such marked sea level minimum was not detected at the monitoring station located north of the Po Delta. Sea level in front of the Venetian lagoon

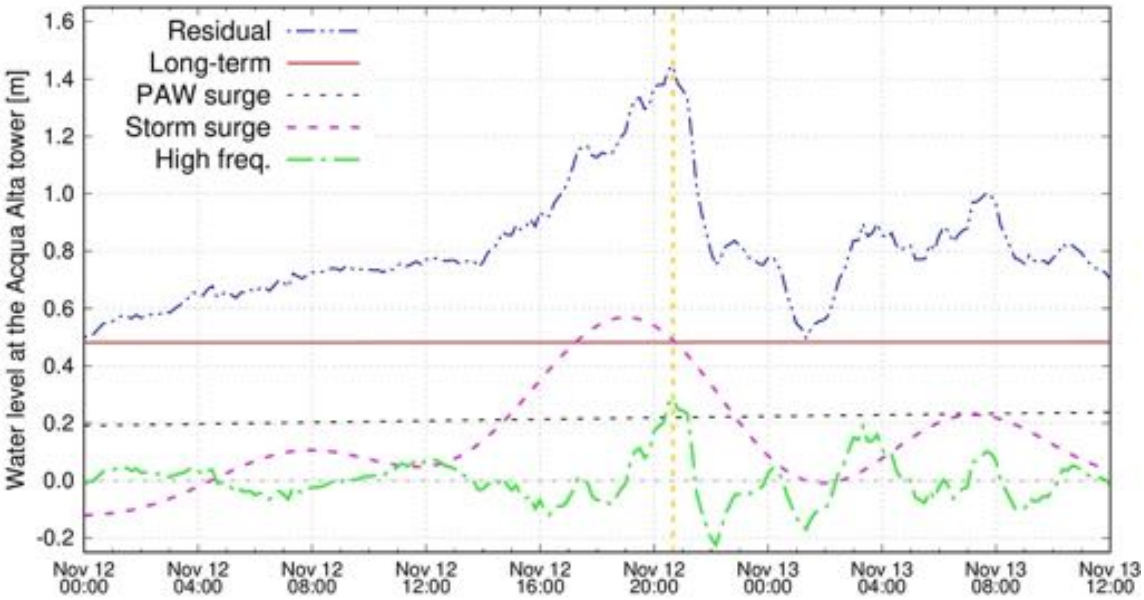

Figure 11: The residual water levels at AAOT and its different components obtained by the spectral analysis of sea level observations. The vertical yellow dashed line highlights the time of the peak of the water level.

rose continuously till around 21:00. After the passage of the barometric pressure minimum and the rotation to south-west, the sea level in the northern Adriatic began to descend rapidly. In the Gulf of Trieste, a well-defined peak was not observed but the sea level remained high for almost 3 hours and then suddenly dropped by almost 1.2 m in 40 minutes. Afterwards, such sea level perturbation produced seiche oscillations of the North Adriatic Sea having a period of about 4 hours (Caloi, 1938; Stravisi, 1977). Summarizing, the L2 perturbation concurred to raise the water level - by superposition to the L1 induced storm surge - along the coast north of the Po Delta, while it supported a fast drop of the sea level south of the Po Delta. Therefore, observations provided evidence of the occurrence of a high-frequency sea level oscillation along the Italian coast generated by the passage of the fast moving perturbation L2.

A wider overview of the high-frequency sea level oscillation is provided by the results of the SHYFEM model forced by the high-resolution MOLOCH-ERA5 meteorological fields. In Fig. 13, we present the residual sea level distribution over the northern Adriatic Sea on 12 November at 20:30 UTC.

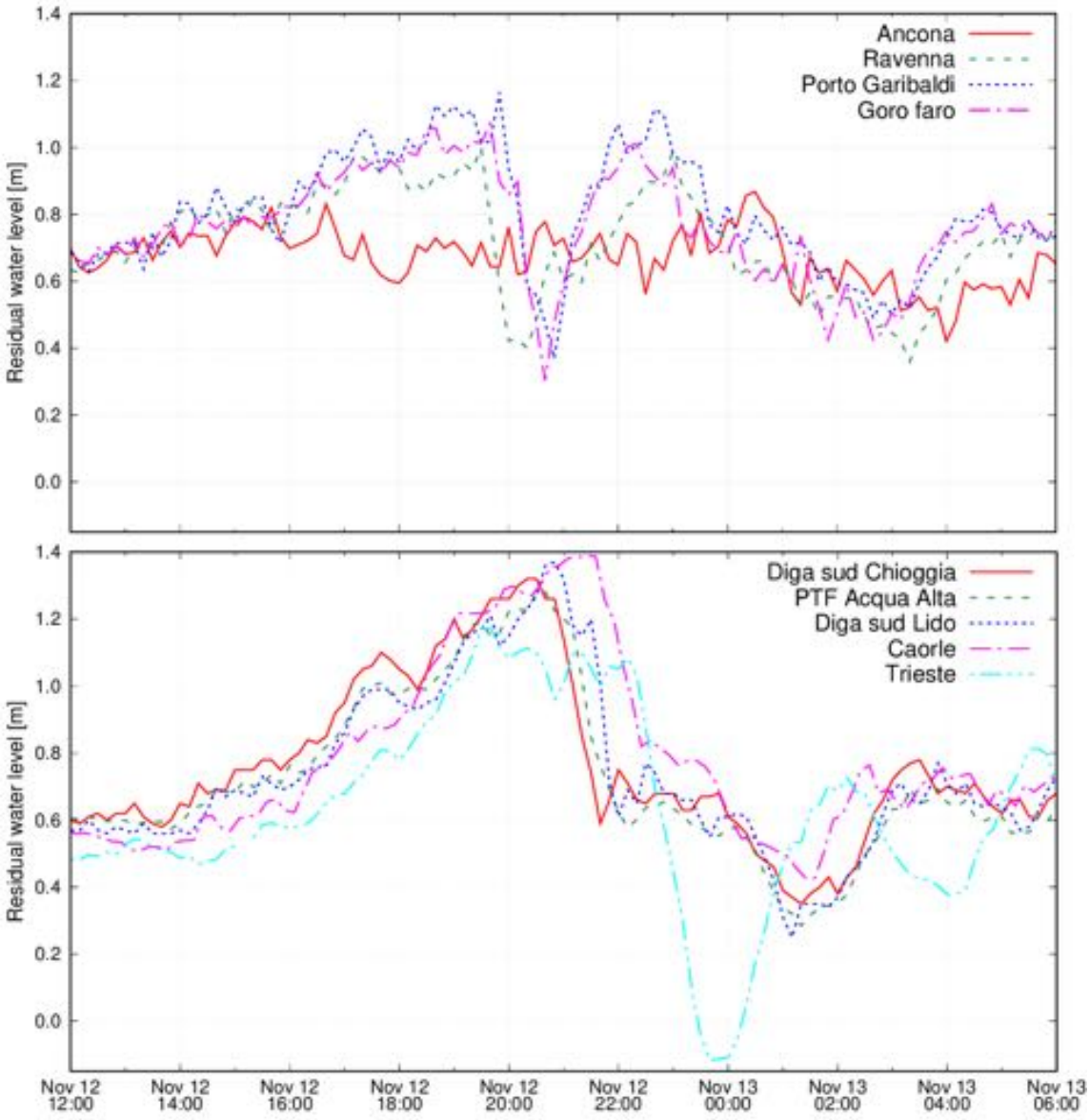

Figure 12: Residual water levels at several stations along the west side of the northern Adriatic coast, north (top panel) and south (bottom panel) of the Po Delta. For comparing the different stations the mean yearly sea level has been removed for each time series.

The model reproduces the sea level variability in the northern Adriatic Sea, with the depression south of the Po Delta and high values in front of the

Lagoon of Venice.

By comparing the simulated residual water levels with the observations, we found that, even if the general dynamics is well reproduced, the model underestimated both the negative and the positive peaks. At the Acqua Alta tower, the model underestimates the observed peak value by 0.19 m (Fig. 14). Likely, this is due to errors, although relatively small, in the reproduction of cyclone L2 (path and intensity) by the meteorological models, since the correct position of the cyclone is very critical in this case. It is interesting and somewhat discouraging to note that, even using the best forcing we can get (local scale model nested on reanalysis), we cannot reproduce the sea level peak.

The water level simulated by forcing the hydrodynamic model with ERA5 data reaches a peak value of 1.02 m (with an underestimation of the storm peak of more than 0.40 m), which is closer to the value obtained considering only the long-term and storm surge MOLOCH forcing. Therefore, from these results, we can deduce that the low-resolution reanalysis ERA5 model correctly described the large-scale perturbation L1, but was not able to reproduce, with a high degree of accuracy, the small-scale atmospheric disturbance L2. A similar mismatch was found in the ECMWF Tco1279 forecasts, which led to a significant underestimation of the water level predicted by the local forecasting institutions (Cavaleri et al., 2020).

As shown in Fig. 5, the low-pressure system L2 propagated in a northwestward direction along the west Adriatic coast on 12 November 2019. The speed of the depression was about 12 m s^{-1} and it propagated along the Italian coast characterized by offshore depths of O(10 m). This means that the depression could be resonantly coupled either to gravity waves (Proudman resonance, Proudman, 1929) or to edge waves (Greenspan resonance, Greenspan, 1956) in the sea. With the aim of checking the occurrence of such a process, we performed numerical simulations forced only by the meteorological fields obtained by applying a high-pass filter (with a cut-off period of 10 hours) to the MOLOCH model results (Fig. 9c). As shown in Fig. 15, the model forced by filtered MSLP fields associated with the L2 perturbation (about 3 hPa depression) simulated a sea level rise in the vicinity of the Lagoon of Venice of 0.12 m, which surpasses the isostatic adjustment to the air pressure variations (the so called inverse barometric effect which amounts to 1 cm per 1 hPa). The four-fold inverse-barometer overshoot is an indication that the atmospheric-ocean resonance was at work on 12 November 2019 and that the L2 depression moving along the Italian coast generated a

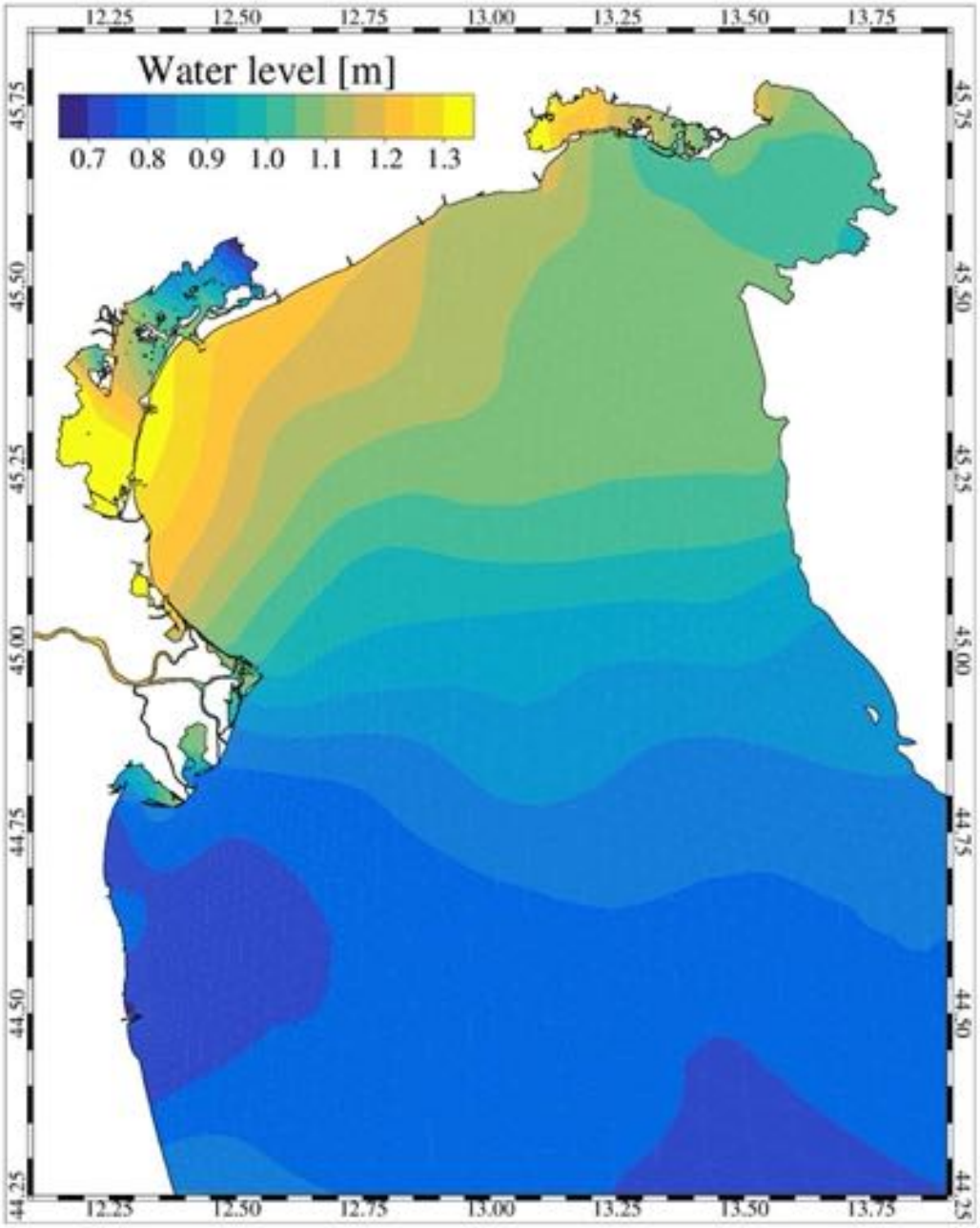

Figure 13: Residual water levels over the northern Adriatic Sea on 12 November at 20:30 UTC as simulated by the SHYFEM model.

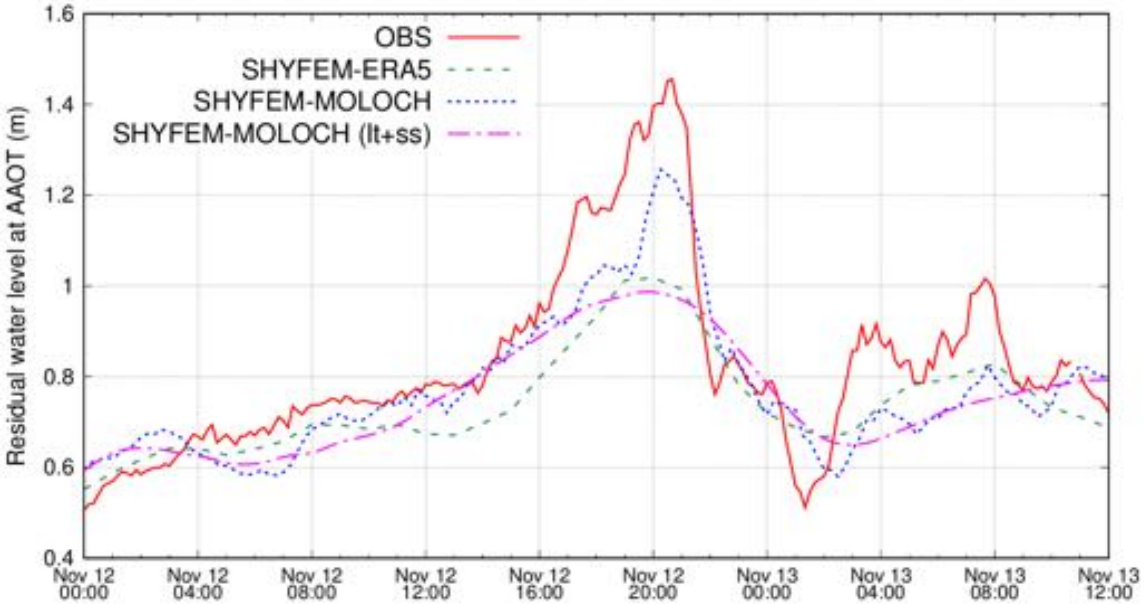

Figure 14: Observed and simulated (using ERA5 and MOLOCH forcing) residual water level at AAOT. The sea level obtained by forcing SHYFEM with the long-term plus storm surge meteorological components is also provided.

meteotsunami-like wave.

Numerical results of the simulation forced by L2 wind and pressure show that, in the shallow waters off the Italian coast, the sea level was influenced not only by the travelling air pressure perturbation but also by the associated winds. The resonant coupling of the travelling wind perturbation related to the local atmospheric depression with gravity or edge waves in the sea was estimated to result in about 0.08 m. The model underestimation of the meteotsunami contribution to the sea level is probably due to the fact that the simulated path and intensity of the L2 perturbation was not perfectly reproduced by the meteorological model.

It should be noted that the difference between the observations and the modelling results forced by the full meteorological contribution amounts to about 0.20 m at AAOT (Fig. 14), whereas the same difference when using only the high-frequency forcing does not surpass 0.10 m at DS Chioggia (Fig. 15). Considering that the wind stress is proportional to the square of the wind speed, such discrepancy is partly due to the way the filters influence the sea level time series when directly applied on the sea level data and when

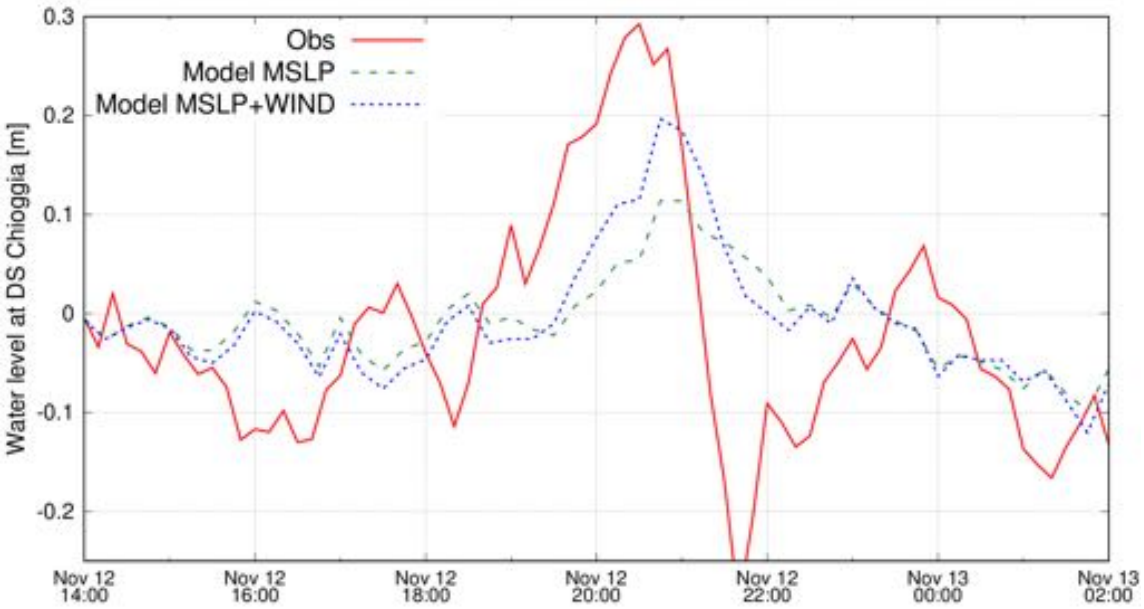

Figure 15: High-frequency signal (period < 10h) of the water level at DS Chioggia as obtained from the spectral analysis of the observations and by the simulation of the SHYFEM model forced by the filtered meteorological fields. Simulations have been carried out with and without considering the wind stress.

applied on the meteorological forcing used to compute the sea levels, and partly due to the underestimation of the storm surge component.

3.3. Sea level evolution within the Lagoon of Venice

The presence of the barrier islands delays and modifies the propagation of sea-level perturbations inside the lagoon, which happens only through the three inlets, and stops almost completely the wind waves. Moreover, shallow coastal systems, like the Lagoon of Venice, promptly respond to the local wind shear stress, which during storms influences the water level (Umgiesser et al., 2004).

On 12 November after the passage of the barometric pressure minimum and the rotation of the wind from south-west, the sea level in the northern Adriatic began to descend rapidly, while the delay of the propagation of the tide in the lagoon made the presence of the most intense south-western gusts coincide with an already critical value of sea level (Fig. 16). These phenomena led to a rapid rise in water levels locally in the lagoon. The maximum sea

level value of 1.89 m above local datum was recorded in Venice at Punta della Salute and occurred at 21:50 UTC with a delay of about an hour compared to the peak of 1.82 m, recorded offshore at the Acqua Alta tower. As for the open sea, the storm tide peak was a consequence of the combination of the maximum meteorological contribution with the lower high tide. An advance or delay of 12 hours of the peak of the event would have led to the overlapping of the meteorological contribution to the higher high tide, with a resulting maximum sea level value of 2.10 m in Venice.

Figure 16 shows a sharp peak of the residual water levels with very fast growing and descending phases. The spectral analysis of the residual levels revealed that such peak could be ascribed to the high-frequency signal determined by the passage of local perturbation L2 and which may be due to the open sea meteotsunami propagating into the lagoon and to the local wind set-up. Similarly to what happened in the open sea (see the data at AAOT in Fig. 11), the storm surge peak associated with the L1 perturbation anticipated the high-frequency peak by about 1 hour.

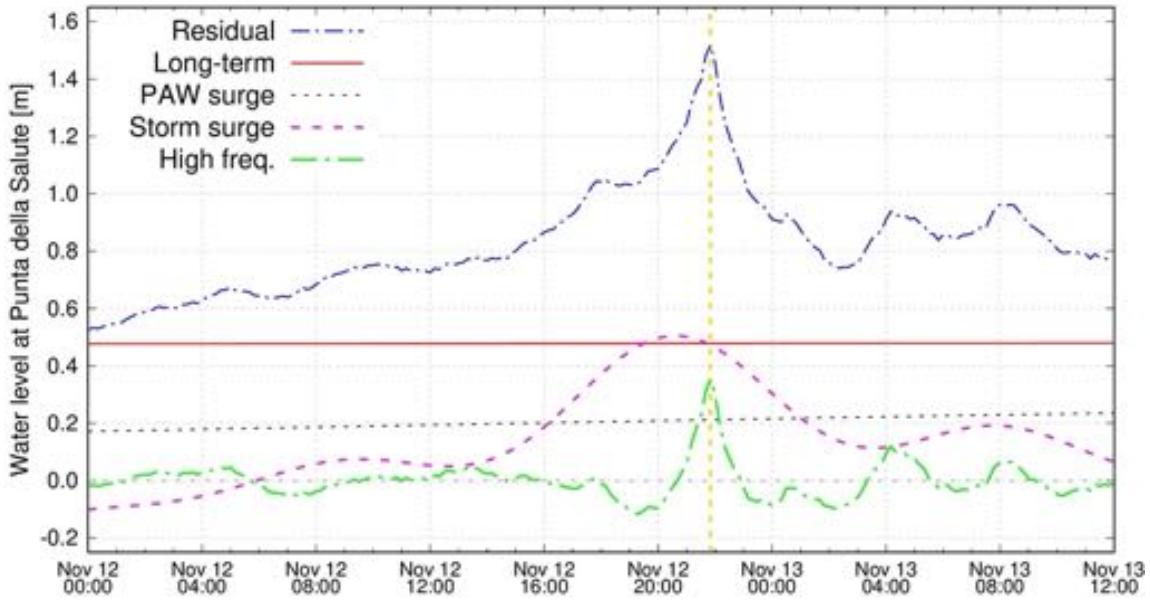

Figure 16: The residual sea level at Punta della Salute and its components obtained by the spectral analysis.

The local meteorological situation, associated with the presence of the L2 vortex that occurred on 12 November resulted in high variability of the

maximum water levels in the lagoon (see Fig. 2 in Cavaleri et al., 2020). The records acquired from the tidal stations inside the lagoon show maximum levels well above 1.70 m only in the open sea and in the historic centre of Venice. A large difference between the levels measured south of the city of Venice (1.89 m at Punta Salute) and to the north (1.73 m at the Misericordia station) occurred in conjunction with the maximum wind from the south-west. In the northern part of the Lagoon, maximum values of less than 1.60 m have been recorded, while in Chioggia the level has stopped at a height of 1.71 m.

The significant wind effect on the water levels inside the Lagoon of Venice was confirmed by the numerical simulations of the lagoon hydrodynamics driven by observed sea levels at the inlets. Two numerical experiments were performed: one forced by observed data of wind and one without wind. As illustrated in Fig. 17a, the strong south-westerly wind generated waves with significant height up to 0.8 m, which hit the southern side of Venice when the water level was maximum. Unfortunately, no wave measurements were available during the storm. The results of the hydrodynamic model confirm the strong sea level gradients in the lagoon registered by the observations, with the highest values found south of the City of Venice and of the bridge that connects it to the mainland (Fig. 17b). The northern part of the lagoon has been preserved from the effects of the storm for several reasons: a) the initial north-east wind; b) the depth, that is on average much smaller than in the central and southern parts of the lagoon, with smaller lagoon channels; c) the southernmost passage of vortex L2. The comparison of the numerical results with the simulation not forced by the wind stress revealed that the strong wind piled up the water toward Venice (up to 0.09 m) determining a remarkable difference in the sea level between the southern and northern sides of the city (Fig. 17c). The simulated sea levels were compared with the available observations confirming the good accuracy of the modelling system with a maximum difference of the peak value of about 2 cm at Punta della Salute (not shown).

Concluding, the peak in the high-frequency signal was so sharp due to the perfect timing of the meteotsunami wave reaching Venice and the maximum wind blowing over the lagoon.

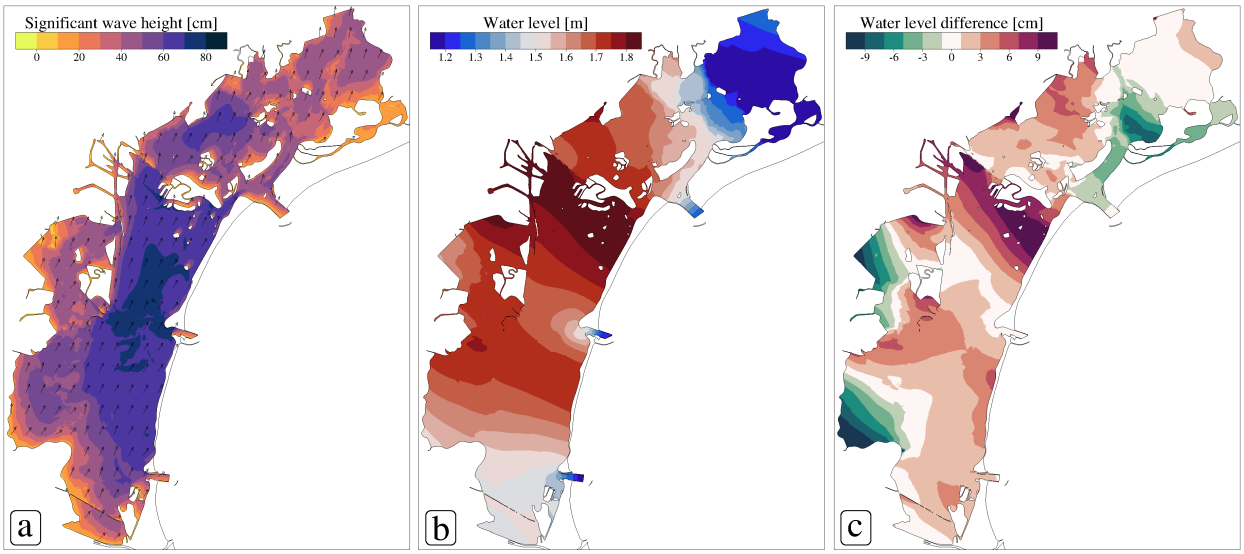

Figure 17: Modelling results inside the Lagoon of Venice. (a) Significant wave height and (b) sea level field at the peak of the storm (12 November at 22:00 UTC) over the Lagoon of Venice. (c) Water level difference between the simulations with and without wind.

4. Large-scale and low-frequency dynamics

In this section, we investigated the meteorological situation in the Mediterranean Sea, which determined a persistent increase of mean sea level in November that reached about 0.30 m in the northern Adriatic Sea. It is well known that in the Mediterranean Sea air pressure and sea level time series show a pronounced low-frequency modulation of amplitudes, with greater amplitudes being observed in winter than in summer (Vilibić et al., 2017, and references therein). Besides the seasonal variability of global atmospheric circulation, there exists substantial wind energy at frequencies which are dominated by planetary atmospheric waves (Penzar et al., 1980; Orlić, 1983). The variations of sea level in the Adriatic at timescales between 10 and 100 days are primarily caused by slowly varying air pressure changes and the associated winds related to the planetary atmospheric waves travelling above the Mediterranean Sea (Pasarić et al., 2000).

Figure 18 shows the November 2019 mean sea level pressure (top panel) and 10m wind (bottom panel) determined by averaging the hourly ERA5 reanalysis fields. The monthly fields reveal a negative pressure anomaly persisting over the western Mediterraneans due to the frequent deepening of

a large-scale trough over the basin and responsible for strong mean easterly winds (with mean speed up to 10 m s^{-1}) prevailing over the Western Mediterranean Sea and south-easterly winds over the Adriatic Sea (with mean speed up to 7 m s^{-1}).

Such meteorological configuration induced a persistent high sea level over the whole Mediterranean Sea throughout the month (Fig. 19). The observed values are considerably surpassing the inverted barometer response, due to the coherent action of air pressure and wind (Pasarić et al., 2000). The November 2019 mean sea level anomaly reached the maximum value above 0.30 m in the northern Adriatic Sea. It is worth noting that the satellite monthly mean anomaly includes the effects of PAW surge, seasonal cycle and inter-annual variability, and is computed with respect to 1993-2012 mean (while observations in Venice are referred to ZMPS). Even if PAW surge oscillations of similar and higher amplitudes have been already observed in the Adriatic Sea (up to 0.7 m as reported in Pasarić and Orlić, 2001), the peculiarity of the November 2019 sea level anomaly resides in its long duration induced by a PAW trough extending over the whole month. In other years, e.g. with the trough lasting from mid-October to mid-November, the PAW surge would be less evident in the monthly mean values.

The long-lasting positive sea level anomaly is confirmed also by the analysis of the historical time series of monthly mean values registered in Venice since 1872 (Fig. 20). The values have been normalised by the annual mean in order to remove the inter-annual variability and highlight the monthly sea level anomaly. It is well known that in the northern Adriatic Sea the sea level has a marked seasonal cycle, strongly related to the atmospheric forcing, with the highest values usually found in November (Bergant et al., 2005), when also most of the flooding events occur (Pasarić and Orlić, 2001). However, the November 2019 anomaly with a value of 0.33 m, ascribed to PAW and the seasonal cycle, falls well outside the 95% confidence interval. Indeed, such a high monthly mean sea level (both as anomaly and absolute values) has never been registered in the northern Adriatic Sea. A similar sea level monthly anomaly was registered in December 1874, when however the annual mean sea level was about 0.45 m lower than today (mostly due to eustasy and subsidence, Carbognin et al., 2004).

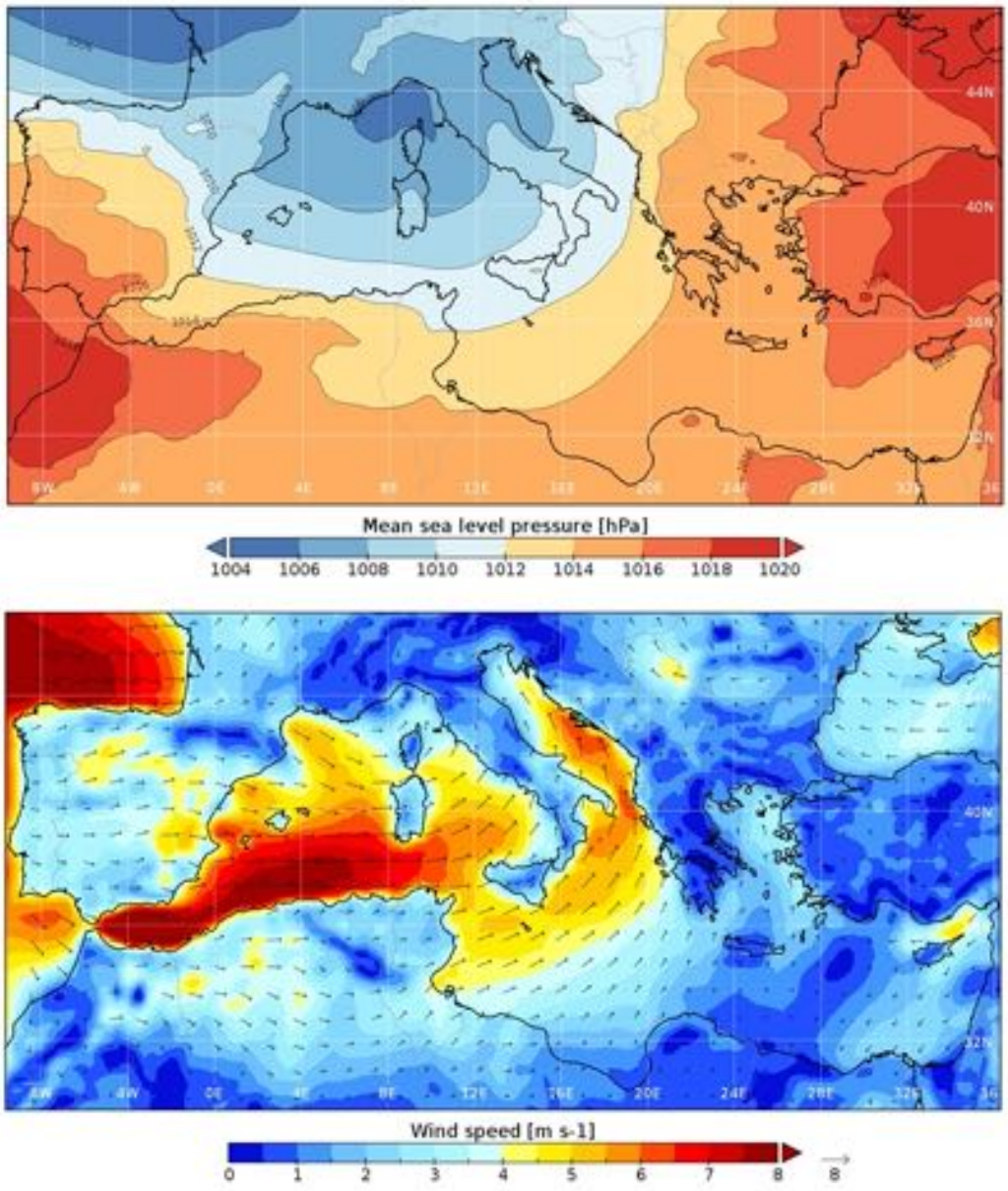

Figure 18: November 2019 monthly mean MSLP (top panel) and 10m wind (bottom panels) fields estimated from ECMWF ERA5 reanalysis.

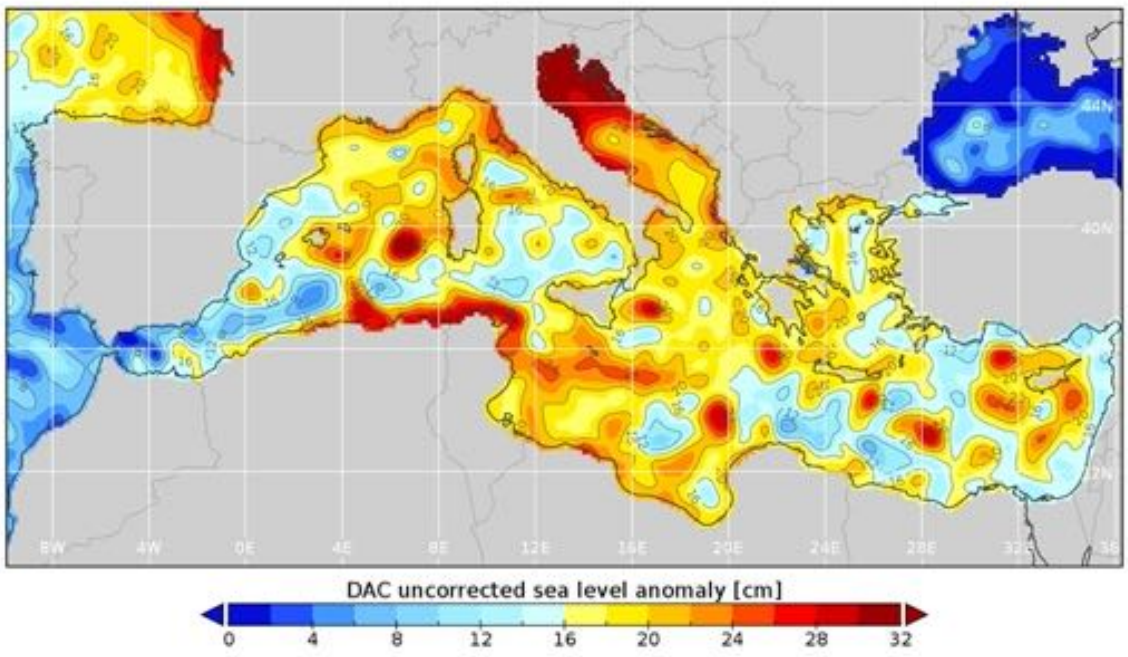

Figure 19: November 2019 mean sea level anomaly (with respect to the 1993-2012 mean) over the Mediterranean Sea obtained by gridded multi-mission altimetry data (DAC uncorrected).

5. A sequence of exceptional flooding events

After the exceptionally high water on 12 November, three successive events with tide level values higher than 1.40 m occurred in just five days (Fig. 21). The meteo-marine data shows that these events were driven by Sirocco wind episodes in succession in the Adriatic Sea on 15 and 17 November, with speed up to 15 m s^{-1}, i.e. significant but not exceptional. Indeed, the meteorological contribution was in the order of 0.7-0.8 m - about half of what was recorded during the 1966 storm - and did not trigger any significant seiche oscillations in the Adriatic Sea (Cerovečki et al., 1997). Similarly to what happened on 12 November, these flood events were determined by the overlapping of the maximum meteorological contribution, the tide peak and a persistent high monthly mean sea level in the northern Adriatic. Finally, another storm surge event occurred on 24 November.

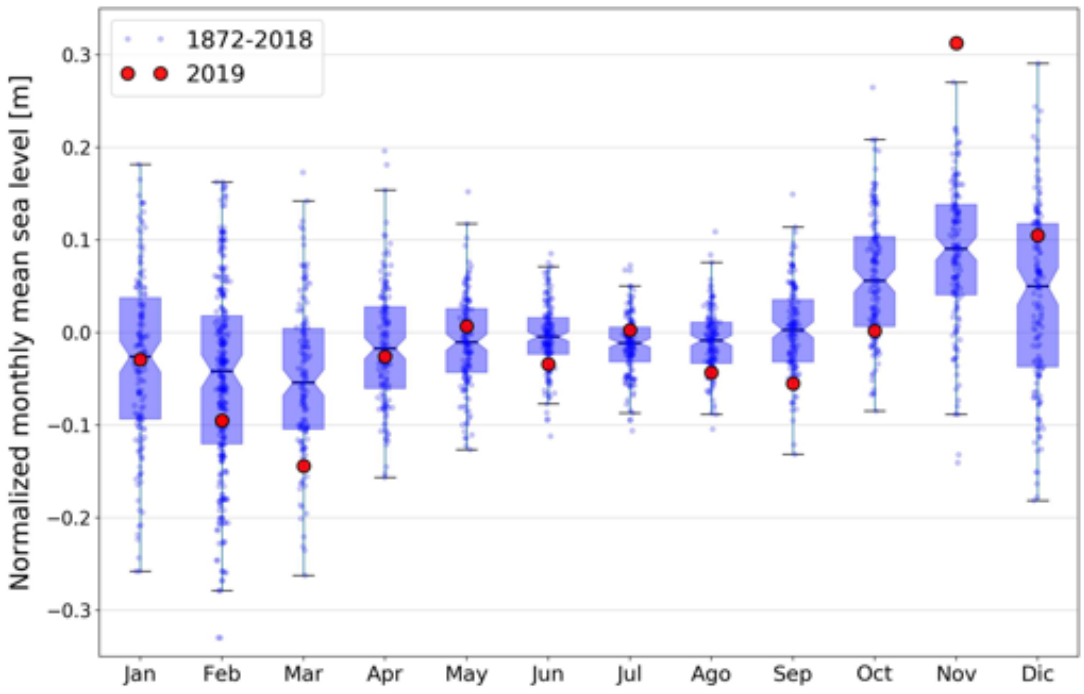

Figure 20: Boxplot of the normalised monthly mean sea levels at Venice for the period 1872-2018 (small blue dots) and 2019 values (red dots).

The meteorological conditions favourable for intense Sirocco wind in the Adriatic and high storm tide peaks in Venice were determined by the repeated deepening of a mid-tropospheric trough over the Mediterranean, slowly evolving eastward, inducing cyclogenesis over the Tyrrhenian Sea.

The flooding events concentrated in the periods 8-18 and 23-29 November during spring tide conditions (Table 2). During the month of November 2019, the sea level in Venice exceeded 40 times the threshold of 0.80 m (the yellow warning level at which Saint Mark's Square get flooded), 15 times the 1.10 m threshold level (the orange warning level at which the MoSE gates would be closed) and 4 times the 1.40 m threshold level (the red warning level which delineates exceptional flooding events). It is to be noted that in November 2019 Venice registered 4 out of the 20 highest water levels in the past 150 years. Such a high frequency of flooding events has never been registered in Venice since 1872 when the official water level monitoring started. In these time frames, Venice was flooded almost every day, thus experiencing something similar to what regular tides will probably be in the next decades

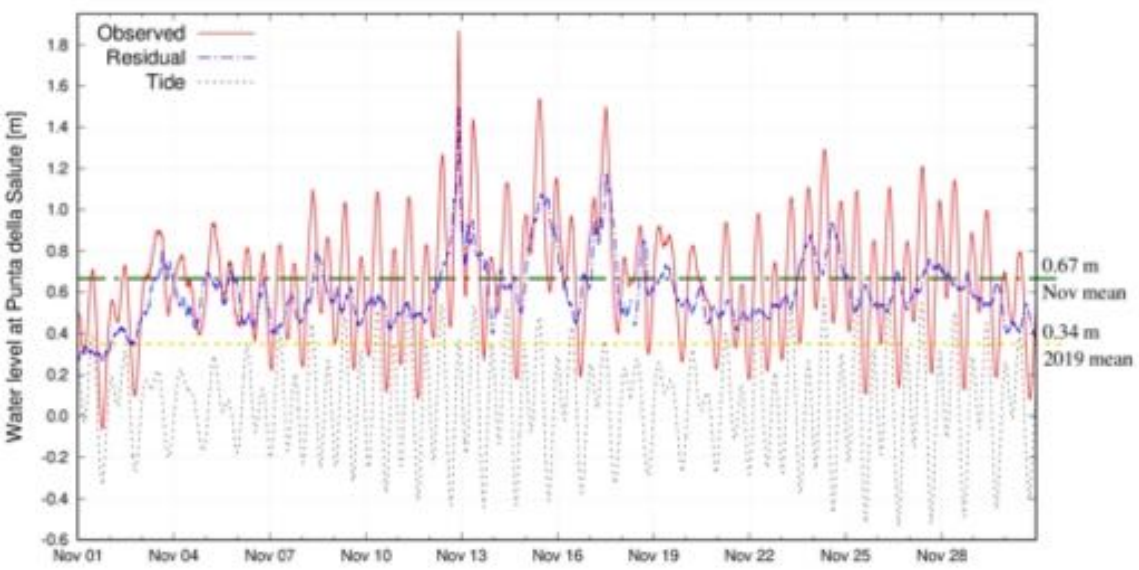

Figure 21: Observed, residual and tidal levels at Venice - Punta della Salute in November 2019. The horizontal yellow dashed and green dot-dashed lines represent the 2019 annual and November monthly mean sea level values, respectively.

with the predicted sea level rise.

Table 2: Number of hours and peaks during the month of November 2019 with sea level in Venice higher than a flooding threshold. The percentage of flooding in the historical centre of the city as a function of the sea level is also reported.

Flooding threshold (m)	*City flooding (%)*	*Hours over threshold*	*Peaks over threshold*
0.8	1	208	40
0.9	2	126	29
1.0	5	78	21
1.1	12	48	15
1.2	28	24	7
1.3	46	14	4
1.4	59	9	4
1.5	70	3	3

6. Discussion

6.1. A combination of local and large-scale factors

The extreme 12 November 2019 flood event in Venice resulted from the exceptional combination of different local and large-scale factors. Contrary to what happened during previous extreme high sea level events that occurred the northern Adriatic Sea (De Zolt et al., 2006), on 12 November the storm surge contribution induced by south-easterly winds was unexceptional. However, during this last event, the peak winds coincided with one of the full moon tidal peaks, while in 1966, 1979 and 2018 the peak of the storm occurred during low tidal conditions (Cavaleri et al., 2019).

As for other flooding events (Pasarić and Orlić, 2001), the low-frequency disturbances of air pressure and wind, associated with PAWs, determined a prolonged interval of high sea level in the northern Adriatic Sea, which provided the long-term precondition for the November 2019 multiple flood events in Venice. As already mentioned above, the amplitude of the PAW surge oscillation was not exceptional, but such a long duration was exceptional for the Adriatic Sea. The long persistence of a trough of PAW over the whole month of November above the western Mediterranean and Adriatic seas could tentatively be interpreted as a consequence of the global warming that is much larger in the polar region than in the equatorial region. This resulted in changes in the atmospheric circulation and, consequently, in an increase of the amplitude and a decrease of the speed of planetary atmospheric waves (Francis and Vavrus, 2012). Moreover, the importance of planetary atmospheric waves would be further enhanced in future, since the frequency of flooding events and the duration of flooding episodes will increase with sea level rise (Orlić and Pasarić, 2005).

In addition to the mentioned processes, the sea level in front of the Lagoon of Venice was enhanced by a meteorological tsunami generated by the local atmospheric disturbance travelling along the north-eastern Adriatic coast. Several meteotsunamis have been identified to be responsible for oscillations of the sea level in the Adriatic Sea (Orlić, 2015). However, even if the first occurrence of atmospherically induced tsunami-like waves was described by (Caloi, 1938) for Trieste, most of the tsunamigenic disturbances travel toward the east-southeast generating meteotsunamis along the Croatian coast, reaching destructive levels within some bays and harbours (Vilibić and Šepić, 2009). Actually, along the Italian coast, we have only a few reports of variations in sea level that exceed by far the equilibrium response to the air

pressure forcing, as a consequence of resonant forcing by an atmospheric perturbation propagating towards the northern Adriatic Sea (Caloi, 1938; Šepić et al., 2012). Therefore, we could reasonably assume that only the open-sea resonance was found to be at work along the Italian coast, whereas both the open-sea and bay/harbour resonances are important in the Croatian archipelago (Vilibić et al., 2017). Possibly super-resonant growth occurred on 12 November since the air pressure disturbance was moving along a gently upward sloping bathymetry and the oceanographic conditions were characterized by counter-currents (ranging from 0.2 to 0.4 m s^{-1}) and high water levels with the falling tide (Williams et al., 2020).

On top of the tide, PAW surge, storm surge and meteotsunami, the sea level in the City of Venice was further raised by the strong south-westerly wind blowing over the lagoon after the passage of the L2 perturbation. Wind and waves hit the southern side of Venice, where Saint Mark's Square and the classical promenade are located. The biggest problem was the relatively high waves, free to proceed above the walking paths, thanks to the exceptionally high sea level. In this way, they were able to throw boats over the shore and collide with the walls of the houses with a run-up effect. Moreover, the wind generated a marked sea level difference between the southern and northern sides of the city, which explains the observed strong flow of water in the canals crossing the city.

6.2. Probability of occurrence of extreme high sea levels

In order to peer into the probability of occurrence of extreme high sea levels, we performed the extreme value analysis of the hourly sea level values observed at Punta della Salute station in the last 80 years (from 1940 to 2019). In order to focus our analysis on tide and non-tidal atmospheric residual (surge), observations were detrended with a 19-year running mean to remove the long-term variability induced by sea level rise, subsidence and non-linear tidal effects of the lunar cycle within the lagoon (Ferrarin et al., 2015). The classical direct method was applied to the original and detrended sea level timeseries, while the joint probability method was used to separate tide and surge. In the latter analysis, the probability density function of the sea level is computed via the convolution integral over an interval which includes all possible tidal and surge levels recorded within the dataset. In simple terms, applying the convolution means that the probability of occurrence of 1.5 m sea level can be seen as the sum of all surge and tidal

probabilities that combine to produce a level of 1.5 m (e.g. a surge of 1 m and a tide of 0.5 m, or a surge of 1.3 m and a tide of 0.2 m).

The highest predicted sea level for the case considered here resulted to be 2.45 m, which is the sum of the maximum surge (1.82 m) and of the highest astronomical tide (0.63 m). It must be noted that the convolution procedure requires statistical independence between the two convoluted variables, so it is of primary importance to understand whether or not they can be treated as such. It is well known that tidal and non-tidal contributions have a certain degree of interaction as they both depend on water depth, so ignoring such dependence could lead to overestimated return levels in very shallow water areas with large tidal excursions where shoaling and other non-linear effects are significant (Horsburgh and Wilson, 2007, and references therein). In the northern Adriatic Sea, the tidal characteristics are only slightly modified by the non-linear tide-surge interaction (Ferrarin et al., 2013). Therefore, although a dependent form of the convolution integral to account for the tide-surge interaction exists (Tawn and Vassie, 1989), we consider the effect of tide on surge propagation negligible and therefore they are treated as two statistically independent variables for practical purposes.

When comparing the extreme 2019 flood event in Venice with the other two major events recorded between 1940 and 2019, i.e. the 1966 and the 1979 high water levels, it is interesting to note the relative importance of the two main contributions whose combined effect produced such exceptionally high levels. Indeed, from Fig. 22 it can be noticed that the 12 November 2019 flood, indicated by a diamond marker, was characterised by a non-exceptional atmospheric surge of 1.19 m combined with a medium-to-high tidal level of 0.36 m. Interestingly, compared to the other two high water events (indicated by triangle and circle markers), this event displays the lowest surge and the highest tidal levels. According to Raicich (2015), the 4 November 1966 event appears to be the most severe one not only since 1872 but also in comparison with any event in the 1751-1769 and 1782-1792 time series.

As can be seen from the convoluted (red) curve, it is clear that the likelihood of having an unfavourable situation similar to the one of 2019, possibly with a more exceptional surge level, is greater than the observed (blue) curve, computed via ordinary-value direct method, might suggest. Indeed, the observed and convoluted curves display similar non-exceedance intervals up to about 15 years, beyond which they then part significantly (difference larger than 0.15 m) as a result of the series of exceptionally high water levels recorded during the 4 November 1966. Thus, on the basis of the convoluted

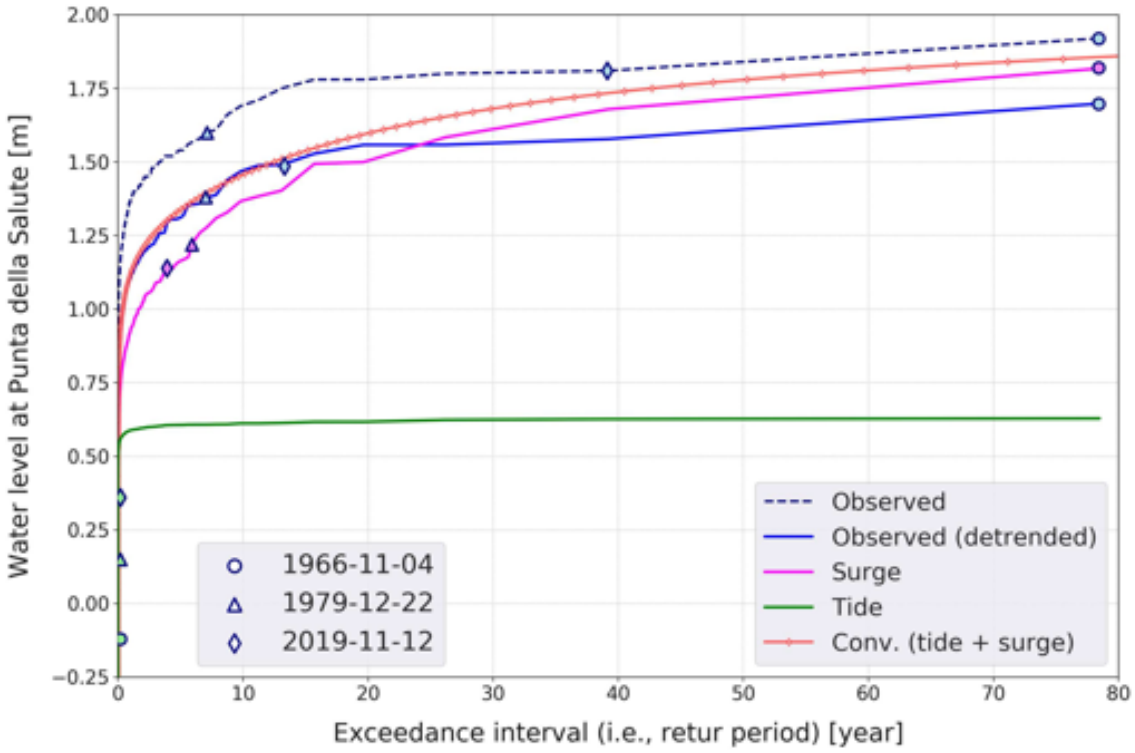

Figure 22: Water level at Punta della Salute for the period 1940-2019. Exceedance interval of hourly observed data (dashed black), detrended observations (blue), astronomical tide (green), surge (detrended observations minus tide, magenta) and convolved (tide and surge, dotted red). The markers indicate the peak values of the three major high water events in Venice (labelled with the date in the bottom-left of the image).

signal, one might expect levels similar to 1966 at least twice as often as recorded even without exceptionally high surge levels. Obviously, the probability of occurrence of future flooding events will increase as the relative sea level rise increases.

The recently completed mobile barriers at the inlet (MOSE project) are now efficiently protecting the city of Venice from storm surges. The first time the MOSE came to action was on 3 October 2020 and it has been operated for a total of 16 events in 2020. Apart from 8 December 2020, when due to an erroneous interpretation of forecast results the MOSE gates have not been closed and the lagoon experienced a water level of 1.38 m, the flooding of the city of Venice was avoided during all other events. However, as shown

in Umgiesser (2020), climate change will increase drastically the number of closures needed. It has been shown that for a SLR of 50 cm a total of 300-400 closures would be needed, i.e., once a day on average.

6.3. Predictability of extreme high sea levels

As noted previously, even using a limited area meteorological model nested into reanalysis fields, we underestimated the sea level peak by about 0.2 m. In this paper, we have highlighted how this storm event can be decomposed and analysed at different spatial and temporal scales. Therefore, to understand its predictability, we will analyse the predictability of its components.

The astronomical tide is a periodic phenomenon that can be predicted with great precision for months, using a good harmonic analysis. There can be interactions with other components of the sea level (e.g. seiches, Bajo et al., 2019), but generally, the error deriving from considering them independent is small in the Adriatic Sea (Ferrarin et al., 2013).

Most of the uncertainty associated with the reproduction of a sea event, like the one of 12 November, resides therefore in the atmospheric contribution. However, the low-frequency components, i.e. seasonal and PAW oscillations, have minimal variations over a few days and therefore do not represent a problem for the sea level short-term forecast, as they can be extrapolated from near real time observations.

The extreme high sea level predictability problem, therefore, focuses on the model's reproduction of the storm surge and high-frequency oscillations (e.g., meteotsunami). Assuming that the errors of the model and of the representation of the physical system are small (Carrassi et al., 2018), the remaining errors are those of the initial state and of the boundary conditions (lateral and surface). The former can be reduced using data assimilation (for the hydrodynamic model), but are only important in the case of pre-existing oscillations (Bajo et al., 2019). The errors in the lateral boundary conditions can be reduced by enlarging the model domain and, in our case, these are out of the Gibraltar Strait, sufficiently far from the northern Adriatic Sea. Therefore, the errors in the surface boundary conditions remain, that is the atmospheric forcings. We have shown how the storm surge in the Adriatic Sea is associated with synoptic-scale phenomena, while the high-frequency oscillation is linked to meso-beta scale phenomena (Orlanski, 1975). Their predictability, therefore, depends on the predictability of these small-scale processes by the atmospheric models. These have the same sources of error

as hydrodynamic models, i.e. the initial state, boundary conditions and model uncertainties. In the last decades, a great effort has been made to improve mesoscale meteorological predictions through the improvement of assimilation techniques, also through the exploitation of large quantities of observations, and by improving numerical models.

Nowadays the large-scale synoptic picture associated with important high sea level events in the northern Adriatic Sea is predictable several days in advance. (Umgiesser et al., 2020). However, even if characteristic favourable synoptic conditions were recognized during meteotsunamis in the Adriatic Sea (the arrival of a temperature front, the presence of a strong jet stream in upper levels and the presence of a low surface air pressure; Šepić et al., 2012), no reliable forecasts of the local tsunamigenic air pressure and wind conditions can be reached from low-resolution (>2 km) mesoscale models (Denamiel et al., 2019). Simplifications such as hydrostaticity and limited spatial and temporal resolution do not make them suitable for the reproduction of beta mesoscale phenomena. Moreover, the capability of reproducing the development of small scale cyclonic vortices as the one affecting the northern Adriatic Sea during this event, requires high-resolution, of the order of 1 km, to correctly describe convective activity and local processes such as air-sea exchanges and interaction with the local orography, which play a key role. It is, therefore, necessary to apply convection-permitting models, possibly nested into mesoscale models. In any case, dealing with smaller scale nonlinear phenomena implies a faster error amplification deriving from the growth of uncertainties of the initial state and the boundary conditions (Lorenz, 1963). The error then propagates in the modelling chain affecting also the prediction of the sea level. This study demonstrated that a relatively small error in the meteorological forecast (the depression trajectory misplaced by about 10-20 km) may produce a considerable error in the sea level prediction which relies on accurate small-scale meteorological forcing. This uncertainty is unavoidable. It can be reduced and it should be dealt with thorough data assimilation and ensemble forecasting techniques, which are still at their beginnings for high-resolution convection-permitting modelling systems (Finn et al., 2020).

7. Conclusions

This work aims to analyse the physics of one of the most extreme flooding events ever recorded in the city of Venice. Its exceptional nature does not

only concern the flooding caused in Venice but also its complexity from a physical point of view. The extreme high sea level recorded in Venice was due to the combination of the following large-scale and local dynamics:

- the in-phase timing between the peak of the atmospheric surge and the lower high astronomical tide;
- a standing low-pressure and wind systems over the Mediterranean Sea - that is associated with planetary atmospheric waves trough extending over the whole month of November - which determined a high monthly mean sea level in the northern Adriatic Sea;
- a deep low-pressure cyclone over the central-southern Tyrrhenian Sea that generated south-easterly winds along the main axis of the Adriatic Sea, pushing waters to the north;
- a fast-moving local depression travelling in the north-westward direction over the Adriatic Sea along the Italian coast, generating a meteotsunami;
- very strong south-westerly winds over the Lagoon of Venice, which led to a rise in water levels and damages to the historic city.

Neither of these contributions was so strong to result in the flooding of the city by its own. Previous extreme high sea levels in the Northern Adriatic Sea (e.g., in 1966, 1979, 2018) were driven by a severe storm surge induced by very strong south-easterly winds blowing over the Adriatic Sea. Each one of these events was in a way a classical one, the difference being mainly in the strength of the storm. Both in 1966 and 2018 a worst disaster was avoided thanks to the astronomical and surge tidal peaks being luckily out of phase. Note that in all these cases the "standard" structure of the storm allowed an extended forecast. A posteriori, using the present know-how and computers, and with only the few data available at the time, also the 1966 surge turned out to be predictable almost one week in advance. This was not the case in the 2019 event. The combination of different independent, each not relevant, but in phase factors led to the dramatic events of 12 November 2019. Particularly the small, but very intense and fast moving low-pressure system was hardly predictable. Indeed, not attempted because being another problem in itself, we wonder if it is possible to estimate the probability, or conversely the return time, of the 2019 overall event. The exceptionality of

this event resides in the coincident superposition of the different mentioned factors. In particular, it is demonstrated that the resonant coupling of the mesoscale atmospheric forcing and the sea made an essential contribution to the event. Also, it is clearly shown how sensitive the simulated/forecasted sea levels are to the small errors in the simulation of mesoscale atmospheric forcing when the resonance phenomena are involved: a small departure from the resonance conditions could result in a large difference in the resulting sea levels.

Acknowledgements

The authors wish to thank the Italian Institute for Environmental Protection and Research (ISPRA), the Tide Forecast and Early Warning Center of the city of Venice (CPSM) and the Agency for Prevention, Environment and Energy of Emilia-Romagna for providing sea level and meteorological data. We wish to thank Prof. Marco Marani for his precious contribution to the extreme value analysis. This work was partially supported by the STREAM project (Strategic development of flood management, project ID 10249186) funded by the European Union under the V A Interreg Italy-Croatia CBC programme. The work done by MO has been supported by Croatian Science Foundation under the project MAUD (IP-2018-01-9849). Paola Malanotte-Rizzoli and two anonymous reviewers have provided useful suggestions to the paper to be ameliorated.

References

Bajo, M., Međugorac, I., Umgiesser, G., Orlić, M., 2019. Storm surge and seiche modelling in the Adriatic Sea and the impact of data assimilation. Quart. J. Roy. Meteor. Soc. 145, 2070–2084. doi:10.1002/qj.3544.

Bellafiore, D., Mc Kiver, W., Ferrarin, C., Umgiesser, G., 2018. The importance of modeling nonhydrostatic processes for dense water reproduction in the southern Adriatic Sea. Ocean Model. 125, 22–28. doi:10.1016/j.ocemod.2018.03.001.

Bergant, K., Sušnik, M., Strojan, I., Shaw, A.G.P., 2005. Sea level variability at Adriatic coast and its relationship to atmospheric forcing. Annales Geophysicae 23, 1997–2010. doi:10.5194/angeo-23-1997-2005.

Buzzi, A., Davolio, S., Malguzzi, P., Drofa, O., Mastrangelo, D., 2014. Heavy rainfall episodes over Liguria in autumn 2011: numerical forecasting experiments. Nat. Hazards Earth Syst. Sci. 14, 1325–1340. doi:10.5194/nhess-14-1325-2014.

Buzzi, A., Speranza, A., 1986. A theory of deep cyclogenesis in the lee of the Alps. Part II: effects of finite topographic slope and height. J. Atmospheric Sci. 43, 2826–2837. doi:10.1175/1520-0469(1986)043<2826:atodci>2.0.co;2.

Buzzi, A., Tibaldi, S., 1978. Cyclogenesis in the lee of the Alps: A case study. Quart. J. Roy. Meteor. Soc. 104, 271–287. doi:10.1002/qj.49710444004.

Caloi, P., 1938. Sesse dell'alto Adriatico con particolare riguardo al Golfo di Trieste. Technical Report 247. Memorie, R. Comitato Talassografico Italiano. In Italian.

Carbognin, L., Teatini, P., Tosi, L., 2004. Eustacy and land subsidence in the Venice Lagoon at the beginning of the new millennium. J. Mar. Syst. 51, 345 – 353. doi:10.1016/j.jmarsys.2004.05.021.

Carrassi, A., Bocquet, M., Bertino, L., Evensen, G., 2018. Data assimilation in the geosciences: An overview of methods, issues, and perspectives. Wiley Interdisciplinary Reviews: Climate Change 9, e535. doi:10.1002/wcc.535.

Carrère, F., Lyar, F., 2006. Modeling the barotropic response of the global ocean to atmospheric wind and pressure forcing - comparisons with observations. Geophys. Res. Lett. 30. doi:10.1029/2002GL016473.

Cavaleri, L., 2000. The oceanographic tower Acqua Alta - activity and prediction of sea states at Venice. Coast. Eng. 39, 29–70. doi:10.1016/S0378-3839(99)00053-8.

Cavaleri, L., Bajo, M., Barbariol, F., Bastianini, M., Benetazzo, A., Bertotti, L., Chiggiato, J., Davolio, S., Ferrarin, C., Magnusson, L., Papa, A., Pezzutto, P., Pomaro, A., Umgiesser, G., 2019. The October 29, 2018 storm in Northern Italy - an exceptional event and its modeling. Prog. Oceanogr. 178, 102178. doi:10.1016/j.pocean.2019.102178.

Cavaleri, L., Bajo, M., Barbariol, F., Bastianini, M., Benetazzo, A., Bertotti, L., Chiggiato, J., Ferrarin, C., Trincardi, F., Umgiesser, G., 2020. The 2019 flooding of Venice and its implications for future predictions. Oceanography 33, 42–49. doi:10.5670/oceanog.2020.105.

Cerovečki, I., Orlić, M., Hendershott, M.C., 1997. Adriatic seiche decay and energy loss to the Mediterranean. Deep Sea Res. Part I 44, 2007–2029. doi:10.1016/S0967-0637(97)00056-3.

Codiga, D.L., 2011. Unified Tidal Analysis and Prediction Using the UTide Matlab Functions. Technical Report 2011-01. Graduate School of Oceanography, University of Rhode Island. Narragansett, RI. URL: http://www.po.gso.uri.edu/~codiga/utide/utide.htm.

Davolio, S., Henin, R., Stocchi, P., Buzzi, A., 2017. Bora wind and heavy persistent precipitation: atmospheric water balance and role of air-sea fluxes over the Adriatic Sea. Q. J. R. Meteorol. Soc. 143, 1165–1177. doi:10.1002/qj.3002.

De Zolt, S., Lionello, P., Nuhu, A., Tomasin, A., 2006. The disastrous storm of 4 November 1966 on Italy. Nat. Hazards Earth Syst. Sci. 6, 861–879. doi:10.5194/nhess-6-861-2006.

Denamiel, C., Šepić, J., Ivanković, D., Vilibić, I., 2019. The Adriatic Sea and Coast modelling suite: Evaluation of the meteotsunami forecast component. Ocean Model. 135, 71 – 93. doi:10.1016/j.ocemod.2019.02.003.

Ferrarin, C., Cucco, A., Umgiesser, G., Bellafiore, D., Amos, C.L., 2010. Modelling fluxes of water and sediment between the Venice Lagoon and the sea. Cont. Shelf Res. 30, 904–914. doi:10.1016/j.csr.2009.08.014.

Ferrarin, C., Roland, A., Bajo, M., Umgiesser, G., Cucco, A., Davolio, S., Buzzi, A., Malguzzi, P., Drofa, O., 2013. Tide-surge-wave modelling and forecasting in the Mediterranean Sea with focus on the Italian coast. Ocean Model. 61, 38–48. doi:10.1016/j.ocemod.2012.10.003.

Ferrarin, C., Tomasin, A., Bajo, M., Petrizzo, A., Umgiesser, G., 2015. Tidal changes in a heavily modified coastal wetland. Cont. Shelf Res. 101, 22 – 33. doi:10.1016/j.csr.2015.04.002.

Ferrarin, C., Valentini, A., Vodopivec, M., Klaric, D., Massaro, G., Bajo, M., De Pascalis, F., Fadini, A., Ghezzo, M., Menegon, S., Bressan, L., Unguendoli, S., Fettich, A., Jerman, J., Ličer, M., Fustar, L., Papa, A., Carraro, E., 2020. Integrated sea storm management strategy: the 29 October 2018 event in the Adriatic Sea. Nat. Hazards Earth Syst. Sci. 20, 73–93. doi:10.5194/nhess-20-73-2020.

Finn, T.S., Geppert, G., Ament, F., 2020. Towards assimilation of wind profile observations in the atmospheric boundary layer with a sub-kilometre-scale ensemble data assimilation system. Tellus A 72, 1–14. doi:10.1080/16000870.2020.1764307.

Francis, J.A., Vavrus, S.J., 2012. Evidence linking Arctic amplification to extreme weather in mid-latitudes. Geophys. Res. Lett. 39, L06801. doi:10.1029/2012GL051000.

Greenspan, H.P., 1956. The generation of edge waves by moving pressure distributions. J. Fluid Mech. 1, 574–592. doi:10.1017/S002211205600038X.

Haigh, I., Nicholls, R., Wells, N., 2010. A comparison of the main methods for estimating probabilities of extreme still water levels. Coast. Eng. 57, 838–849.

Hersbach, H., Bell, B., Berrisford, P., Hirahara, S., Horànyi, A., Munoz-Sabater, J., Nicolas, J., Peubey, C., Radu, R., Schepers, D., Simmons, A., Soci, C., Abdalla, S., Abellan, X., Balsamo, G., Bechtold, P., Biavati, G., Bidlot, J., Bonavita, M., De Chiara, G., Dahlgren, P., Dee, D., Diamantakis, M., Dragani, R., Flemming, J., Forbes, R., Fuentes, M., Geer, A.,

Haimberger, L., Healy, S., Hogan, R.J., Hólm, E., Janisková, M., Keeley, S., Laloyaux, P., Lopez, P., Lupu, C., Radnoti, G., de Rosnay, P., Rozum, I., Vamborg, F., Villaume, S., Thépaut, J.N., 2020. The era5 global reanalysis. Quart. J. Roy. Meteorol. Soc. 146, 1999–2049. doi:10.1002/qj.3803.

Holton, J.R., 2004. An Introduction to Dynamic Meteorology (Fourth Edition). Elsevier, Amsterdam, The Netherlands, 535 pp.

Horsburgh, K.J., Wilson, C., 2007. Tide-surge interaction and its role in the distribution of surge residuals in the North Sea. J. Geophys. Res. 112. doi:10.1029/2006JC004033.

Hubbard, M.E., Nikiforakis, N., 2003. A three-dimensional, adaptive, Godunov-type model for global atmospheric flows. Mon. Wea. Rev. 131, 1848–1864. doi:10.1175//2568.1.

Lionello, P., Barriopedro, P., Ferrarin, C., Nicholls, R., Orlić, M., Raicich, F., Reale, M., Umgiesser, G., Vousdoukas, M., Zanchettin, D., 2020. Extremes floods of Venice: characteristics, dynamics, past and future evolution. Nat. Hazards Earth Syst. Sci. Discuss. -, –. doi:10.5194/nhess-2020-359.

Lionello, P., Cavaleri, L., Nissen, K., Pino, C., Raicich, F., Ulbrich, U., 2012. Severe marine storms in the Northern Adriatic: Characteristics and trends. Phys. Chem. Earth., Parts A/B/C 40-41, 93 – 105. doi:10.1016/j.pce.2010.10.002.

Lionello, P., Mufato, R., Tomasin, A., 2005. Sensitivity of free and forced oscillations of the Adriatic Sea to sea level rise. Clim. Res. 29, 23 – 39. doi:10.3354/cr029023.

Lorenz, E.N., 1963. Deterministic nonperiodic flow. J. Atmos. Sci. 20, 130 – 141.

Madricardo, F., Foglini, F., Kruss, A., Ferrarin, C., Pizzeghello, N.M., Murri, C., Rossi, M., Bajo, M., Bellafiore, D., Campiani, E., Fogarin, S., Grande, V., Janowski, L., Keppel, E., Leidi, E., Lorenzetti, G., Maicu, F., Maselli, V., Mercorella, A., Gavazzi, G.M., Minuzzo, T., Pellegrini, C., Petrizzo, A., Prampolini, M., Remia, A., Rizzetto, F., Rovere, M., Sarretta, A., Sigovini, M., Sinapi, L., Umgiesser, G., Trincardi, F., 2017. High-resolution multibeam and hydrodynamic datasets of tidal channels and inlets of the Lagoon of Venice. Sci. Data 4. doi:10.1038/sdata.2017.121.

Malguzzi, P., Grossi, G., Buzzi, A., Ranzi, R., Buizza, R., 2006. The 1966 "century" flood in Italy: A meteorological and hydrological revisitation. J. Geophys. Res. 111. doi:10.1029/2006JD007111.

Markowsky, P., Richardson, Y., 2010. Mesoscale Meteorology in Midlatitudes. Wiley-Blackwell, Chichester, UK, 407 pp.

Mazas, F., Kergadallan, X., Garat, P., Hamm, L., 2014. Applying POT methods to the Revised Joint Probability Method for determining extreme sea levels. Coast. Eng. 91, 140–150.

Međugorac, I., Orlić, M., Janeković, I., Pasarić, Z., Pasarić, M., 2018. Adriatic storm surges and related cross-basin sea-level slope. J. Mar. Syst. 181, 79–90. doi:10.1016/j.jmarsys.2018.02.005.

Orlanski, I., 1975. A rational subdivision of scales for atmospheric processes. Bull. Amer. Meteor. Soc. 56, 527–530.

Orlić, M., 1983. On the frictionless influence of planetary atmospheric waves on the Adriatic sea level. J. Phys. Oceanogr. 13, 1301–1306. doi:10.1175/1520-0485(1983)013<1301:OTFIOP>2.0.CO;2.

Orlić, M., 2001. Anatomy of sea level variability - an example from the Adriatic, in: El-Hawary, F. (Ed.), The Ocean Engineering Handbook, CRC Press, Boca Raton (USA). pp. 1.1–1.14.

Orlić, M., 2015. The first attempt at cataloguing tsunami-like waves of meteorological origin in Croatian coastal waters. Acta Adriat. 56, 83 – 96.

Orlić, M., Pasarić, M., 2005. Will the future sea-level rise result in the northern Adriatic flooding episodes of longer duration?, in: Lasserre P., Viaroli P., C.P.W.P.L. (Ed.), Proceedings of the Lagoons and Coastal Wetlands in the global change context: impacts and management issues. Venice.

Pasarić, M., Orlić, M., 2001. Long-term meteorological preconditioning of the North Adriatic coastal floods. Cont. Shelf Res. 21, 263 – 278. doi:10.1016/S0278-4343(00)00078-9.

Pasarić, M., Pasarić, Z., Orlić, M., 2000. Response of the Adriatic sea level to the air pressure and wind forcing at low frequencies (0.01-0.1 cpd). J. Geoph. Res. 105, 11423–11439. doi:10.1029/2000JC900023.

Pasarić, Z., Belušić, D., Chiggiato, J., 2009. Orographic effects on meteorological fields over the Adriatic from different models. J. Mar. Syst. 78, S90 – S100. doi:10.1016/j.jmarsys.2009.01.019.

Penzar, B., Orlić, M., Penzar, I., 1980. Sea-level changes in the Adriatic as a consequence of some wave occurrences in the atmosphere. Thalassia Jugosl. 16, 51–77.

Polli, S., 1960. La propagazione delle maree nell'Alto Adriatico. Technical Report 370. Istituto Sperimentale Talassografico, Trieste. In Italian.

Proudman, J.F.R.S., 1929. The effects on the sea of changes in atmospheric pressure. Geophys. Suppl. Month. Notices. R. Astron. Soc. 2, 197–209.

Pugh, D.T., Vassie, J.M., 1980. Applications of the joint probability method for extreme sea level computations. Proc. Instn. Civ. Engrs., Part 2 69, 959–975.

Pujol, M.I., Faugère, Y., Taburet, G., Dupuy, S., Pelloquin, C., Ablain, M., Picot, N., 2016. DUACS DT2014: the new multi-mission altimeter data set reprocessed over 20 years. Ocean Sci. 12, 1067–1090. doi:10.5194/os-12-1067-2016.

Raicich, F., 2015. Long-term variability of storm surge frequency in the venice lagoon: an update thanks to 18th century sea level observations. Nat. Hazards Earth Syst. Sci. 15, 527–535. doi:10.5194/nhess-15-527-2015.

Roland, A., Cucco, A., Ferrarin, C., Hsu, T.W., Liau, J.M., Ou, S.H., Umgiesser, G., Zanke, U., 2009. On the development and verification of a 2d coupled wave-current model on unstructured meshes. J. Mar. Syst. 78, Supplement, S244–S254. doi:10.1016/j.jmarsys.2009.01.026.

Šepić, J., Vilibić, I., Strelec Mahović, N., 2012. Northern Adriatic meteorological tsunamis: Observations, link to the atmosphere, and predictability. J. Geophys. Res. Oceans 117. doi:10.1029/2011JC007608.

Sotillo, M.G., Cailleau, S., Lorente, P., Levier, B., Aznar, R., Reffray, G., Amo-Baladron, A., Chanut, J., Benkiran, M., Alvarez-Fanjul, E., 2015. The MyOcean IBI Ocean Forecast and Reanalysis Systems: operational products and roadmap to the future Copernicus Service. J. Oper. Oceanogr. 8, 63–79. doi:10.1080/1755876X.2015.1014663.

Speranza, A., Buzzi, A., Trevisan, A., Malguzzi, P., 1985. A theory of deep cyclogenesis in the lee of the Alps. Part I: modifications of baroclinic instability by localized topography. J. Atmospheric Sci. 42, 1521–1535. doi:10.1175/1520-0469(1985)042<1521:atodci>2.0.co;2.

Stravisi, F., 1977. Bora driven circulation in northern Adriatic. Boll. Oceanol. Teor. Appl 19, 95–102.

Tawn, J.A., Vassie, J.M., 1989. Extreme sea levels: the joint probabilities method revisited and revised. Proc. Instn. Civ. Engrs., Part 2 87, 429–442.

Tsimplis, M.N., Proctor, R., Flather, R.A., 1995. A two-dimensional tidal model for the Mediterranean Sea. J. Geophys. Res. Oceans 100, 16223–16239. doi:10.1029/2006JC004033.

Umgiesser, G., 2020. The impact of operating the mobile barriers in Venice (MOSE) under climate change. J. Nat. Conserv. 54, 125783. doi:10.1016/j.jnc.2019.125783.

Umgiesser, G., Ferrarin, C., Bajo, M., Tosoni, A., Papa, A., Ferla, M., Lionello, P., Zanchettin, D., Bertin, X., Fortunato, A., Haigh, I.D., Orlić, M., Woge Nielsen, J., 2020. The prediction of floods in Venice: methods, models and uncertainty. Nat. Hazards Earth Syst. Sci. Discuss. -, –. doi:10.5194/nhess-2020-361.

Umgiesser, G., Ferrarin, C., Cucco, A., De Pascalis, F., Bellafiore, D., Ghezzo, M., Bajo, M., 2014. Comparative hydrodynamics of 10 Mediterranean lagoons by means of numerical modeling. J. Geophys. Res. Oceans 119, 2212–2226. doi:10.1002/2013JC009512.

Umgiesser, G., Melaku Canu, D., Cucco, A., Solidoro, C., 2004. A finite element model for the Venice Lagoon. Development, set up, calibration and validation. J. Mar. Syst. 51, 123–145. doi:10.1016/j.jmarsys.2004.05.009.

Vilibić, I., Denamiel, C., Zemunik, P., Monserrat, S., 2020. The Mediterranean and Black Sea meteotsunamis: an overview. Nat. Hazards doi:10.1007/s11069-020-04306-z.

Vilibić, I., Šepić, J., 2009. Destructive meteotsunamis along the eastern Adriatic coast: Overview. Phys. Chem. Earth., Parts A/B/C 34, 904 – 917. doi:10.1016/j.pce.2009.08.004.

Vilibić, I., Šepić, J., Pasarić, M., Orlić, M., 2017. The Adriatic Sea: a long-standing laboratory for sea level studies. Pure Appl. Geophys. 174, 3765–3811.

Williams, D.A., Horsburgh, K.J., Schultz, D.M., Hughes, C.W., 2020. Proudman resonance with tides, bathymetry and variable atmospheric forcings. Nat. Hazards doi:10.1007/s11069-020-03896-y.

Woodworth, P.L., Melet, A., Marcos, M., Ray, D.R., Wöppelmann, G., Sasaki, Y.N., Cirano, M., Hibbert, A., Huthance, J.M., Monserrat, S., Merrifield, M.A., 2019. Forcing factors affecting sea level changes at the coast. Surv. Geophys. 40, 1351–1397. doi:10.1007/s10712-019-09531-1.

Declaration of interests

☒The authors declare that they have no known competing financial interests or personal relationships that could have appeared to influence the work reported in this paper.

☐The authors declare the following financial interests/personal relationships which may be considered as potential competing interests: